PHILOSOPHICAL TRANSACTIONS OF THE ROYAL SOCIETY A MATHEMATICAL, PHYSICAL & ENGINEERING SCIENCES

An Experimental Determination of the Fermi Surface in Copper

A. B. Pippard

Phil. Trans. R. Soc. Lond. A 1957 **250**, 325-357
doi: 10.1098/rsta.1957.0023

AN EXPERIMENTAL DETERMINATION OF THE FERMI SURFACE IN COPPER

By A. B. PIPPARD, F.R.S.

Institute for the Study of Metals, University of Chicago, U.S.A.
and Royal Society Mond Laboratory, University of Cambridge

(*Received* 12 *April* 1957)

CONTENTS

Measurements have been made of the variation with crystal orientation of the anomalous skin resistance of plane surfaces of pure copper at low temperatures and at a frequency of 22700 Mc/s. The resistance is related to the geometrical form of the Fermi surface, and a surface is determined which has the correct shape to account for the experimental results. It is believed that there is no other solution which would give equally good agreement. As determined, the surface, which holds one electron per atom, will not quite fit into the Brillouin zone, overlapping in the (111) directions where the zone boundary is closest to the origin. From an examination of simple models it is concluded that probably there is contact with the zone boundary over small areas around these points, and the energy gap across these boundaries is estimated to be about $7\frac{1}{2}$ eV. Apart from extension to the boundaries in the (111) directions the Fermi surface is more or less spherical. An estimate is made of the Fermi velocity and its variations over the surface, from which it is concluded that the electronic specific heat should lie between 1·7 and 1·9 times that of a free-electron model of copper. The experimental value is 1·38, and it is tentatively suggested that the discrepancy may find an explanation in the theory of Bohm & Pines. Various transport phenomena are briefly discussed, but no reliable evidence is discovered bearing directly on the shape of the Fermi surface. It is concluded that the method, though laborious in interpretation, may be applied with advantage to other simple metals such as silver and gold.

Introduction

It has been shown (Sondheimer 1954; Pippard 1954, hereafter referred to as I) that by a study of the anomalous skin effect in single crystals of a pure metal, information may be obtained about the geometrical form of the Fermi surface, uncomplicated by the need for knowledge of electronic velocity, relaxation time or other parameters. The results of the theory may be summarized as follows. If a flat plate be cut from a single crystal of the

Vol. 250. A. 979. (Price 10*s*. 6*d*.) 41 [Published 12 December 1957

metal and the surface resistance R be measured at a high angular frequency ω, in general R will vary in tensorial fashion as the direction of current flow in the plane of the surface is altered; for suitably chosen axes in the surface,

$$R = R_x \cos^2\phi + R_y \sin^2\phi, \tag{1}$$

in which ϕ is the angle between the direction of current flow and the x axis, and R_x and R_y are the principal surface resistances. It is R_x and R_y which may be related to the geometry of the Fermi surface; let us consider R_x. In momentum space (the momentum $\mathbf{p}$ is defined as $\hbar\mathbf{k}$, where $\mathbf{k}$ is the wave vector of the electronic state considered) the occupied electronic states may extend over several Brillouin zones, so that on the reduced zone diagram the Fermi surface, marking the limit of occupied states at the absolute zero, may consist of a number of distinct sheets, which may be open or closed. We now define Cartesian axes which apply to both real and momentum spaces, x being the direction of current flow, y normal to x in the plane of the specimen and z normal to the plane of the specimen. On the Fermi surface we may describe the 'effective zone', which is the locus of all points at which the normal to the Fermi surface is perpendicular to the z axis. It is the electrons lying near the effective zone which contribute most largely to the current under extreme anomalous conditions, when the free path is much greater than the skin depth, since it is only these which can execute a substantial fraction of a free path within the region occupied by the field. If at any point on the effective zone the radius of curvature of the Fermi surface in a plane normal to the y axis is ρ_y, then in the limit of infinite free path

$$R_x = \frac{\sqrt{3}}{2}\left\{\frac{\pi\omega^2\hbar^3}{e^2\int|\rho_y|\,\mathrm{d}y}\right\}^{\frac{1}{3}}, \tag{2}$$

the integral being taken over the effective zone. Similarly

$$R_y = \frac{\sqrt{3}}{2}\left\{\frac{\pi\omega^2\hbar^3}{e^2\int|\rho_x|\,\mathrm{d}x}\right\}^{\frac{1}{3}}, \tag{3}$$

where ρ_x is the radius of curvature of the Fermi surface at a point on the effective zone, in a plane normal to the x axis.

It will be seen from (2) and (3) that there is a possibility of using experimental determinations of R_x and R_y for a number of specimens cut at different angles to the crystal axes to discover how the curvature varies over the Fermi surface, and hence to construct the surface itself. But because the curvature appears only in integral form, and the integral is in any case to be taken around a path which can only be determined once the shape of the Fermi surface is known, there is plenty of scope left for ambiguities of interpretation. This is particularly true in a complex metal whose Fermi surface may consist of many sheets, for the contributions to the integrals from each zone are not distinguishable, and one could not easily be certain that a set of surfaces consistent with the experimental results was a unique solution. It is for this reason that Fawcett's (1955) application of the method to tin does not carry complete conviction, however plausible his set of Fermi surfaces may appear. For such a complex metal other methods of investigation hold out

more promise, particularly the de Haas–van Alphen effect in high fields (Shoenberg 1957), though the anomalous skin effect may eventually prove a valuable tool in fixing details of the shape once its general form has been found.

There is, however, much more hope of a successful application of the anomalous skin effect to a monovalent metal in which the Fermi surface may be presumed to consist of only a single sheet, and additional incentive for such an investigation is provided by the lack of success which has so far attended all attempts to observe the de Haas–van Alphen effect in these metals. Copper was chosen for the present study, on account of its metallurgical convenience.

Experimental method

For reliable results to be obtained the crystals used must be made of high-purity copper, so that at low temperatures the free path of the electrons may rise to values much greater than the skin depth, which is about 10^{-5} cm. Since in copper, according to Chambers (1952), the ratio of conductivity to free path, σ/l, is $15{\cdot}4 \times 10^{10}\ \Omega^{-1}\ \mathrm{cm}^{-2}$ it is necessary in order to achieve a value for l of 10^{-3} cm to have σ at least as great as $1{\cdot}54 \times 10^{8}$, about 90 times the room-temperature value. The copper actually used, supplied by the American Smelting and Refining Company, had a residual resistance after crystallization about 1/200 of the room-temperature value. Thus the ratio of free path to skin depth was about 220, quite sufficient to bring the surface resistance close to the limiting value for infinite free path. The finished specimens consisted of circular disks $1\frac{1}{4}$ in. in diameter and about $\frac{1}{8}$ in. thick, flat and electropolished on one face. As the success of the experiments depends on the state of perfection of the surface, a somewhat detailed description will now be given of the preparation of the specimens.

Single crystals of copper $1\frac{3}{8}$ in. in diameter and about 4 in. long were made by casting carefully degassed copper into pure graphite moulds *in vacuo*, and then slowly withdrawing the melt from the furnace. Three such crystals were made, mounted with plaster in thick-walled brass tubes, and oriented crystallographically by X-ray reflexion. The specimens were cut from the crystals at the desired orientations by means of a high-speed abrasive wheel. The original cuts were made to produce rather thick elliptical disks; they were mounted with wax on a mandrel and very slowly and carefully turned down to circular shape and something like the thickness required. It was verified after this procedure that they were still single crystals. No further treatment was given to the machined face, which was not used for measurement. The other face was etched with nitric acid until about 0·02 in. had been removed. X-ray examination at this stage gave a back-reflexion Laue pattern that was extremely sharp and free from scattering, indicating that the etching was sufficient to remove the mechanically deformed surface layer. It was now necessary to produce a smoothly polished surface without introducing any more deformation. The etched surface was gently ground flat with 600 grit Carborundum, and then alternately lightly etched and very gently polished until a good lapped surface was achieved. At this stage the X-ray pattern was distinctly impaired, but the original high quality was restored by electropolishing. The polishing bath was a mixture of 50 % each of syrupy phosphoric acid and water, and the specimen was polished in a horizontal position below a perforated cathode. The polishing was carried out in cycles of 3 min each, the specimen being washed but not mechanically polished between cycles. After the

second cycle the X-ray pattern was restored to its original fine quality, and each specimen was given a third cycle of polishing. After washing and drying, the specimens were stored in a desiccator.

It may be remarked that experiments on the anomalous skin effect require that the surface layer, 10^{-5} cm thick, into which the field penetrates, shall be smooth on the scale of 10^{-5} cm and shall have an electronic free path as large as in the bulk of the material. The latter necessity imposes a stringent condition on the state of the surface layer, and it is probable that vestiges of mechanical deformation too small to affect the X-ray pattern could reduce the free path to a serious extent. Thus the examinations of the specimen described above, though useful as general tests of the success of the polishing technique, are not adequate to ensure that the surface layer is really equivalent to a slice of the bulk material. A better test is provided by examining the effect of further electropolishing on the measured values of the surface resistance. Two specimens, α and λ (see table 1), were given two further cycles of electropolishing after measurement, without further mechanical polishing of course, and were then found to have suffered no significant change in R. It is probable, therefore, that all residual mechanical strain was eliminated in the treatment of the surface.

TABLE 1

specimen		θ	$10^2 R_x\,(\Omega)$	$10^2 R_y\,(\Omega)$
series 1	α	0	0·611 0·624	0·655 0·624*
	β	12	0·920	0·629
	γ	22	1·065	0·712
	δ	33	0·925	0·775
	ϵ	45·3	0·873	0·845
	ζ	54·7	0·958	0·972
	η	62	0·765	0·965†
	θ	70·7	0·885	0·991
	κ	79·5	1·110§	—
	λ	90	1·129 1·092	1·010 1·033*
series 2	α	0	0·629 (mean)‡	
	μ	8·4	0·859	0·852
	ν	22·5	0·981	1·050
	λ	45	1·022 (mean)	1·111 (mean)‡

* The second pairs of readings for α and λ were taken after fresh electropolishing of the surface.

† The measurements were taken in error at 30° to the x and y axes, giving values for R of 0·815 and 0·915, from which the values for R_x and R_y were derived.

‡ Taken from values given in series 1. Note that for λ R_x and R_y become interchanged, compared with series 1.

§ This point was taken on a typical Chicago summer day, when humidity deranged the d.c. measurements. It is regarded as unreliable, and is not used.

The smoothness of the surface may be crudely tested by microscopic examination with strong oblique illumination. Small-scale roughness shows up as a milky appearance, as a result of diffuse scattering by the asperities, but all the specimens used gave an intensely dark field; there was thus no significant roughness on the scale of the wavelength of light. Electron micrography of a replica of one surface failed to reveal any structure of magnitude comparable with 10^{-5} cm. It will, therefore, be assumed that the results obtained for the resistance refer to smooth unstrained surfaces. In particular, differences between R_x and R_y for a given surface are to be ascribed to anisotropy of the electron distribution in momentum space and not simply to a grained structure of the surface.

The measurement of the surface resistance was made at a frequency of 22700 Mc/s (wavelength 1·32 cm), by means of a calorimetric technique using the apparatus shown diagrammatically in figure 1. The principle is similar to that of Fawcett's (1955) study of tin, but employs certain constructional simplifications which merit description. The specimen A is mounted below the end of a rectangular waveguide B, close to, but not touching, a flat copper flange C in which are three circular grooves about one-quarter wavelength deep to prevent escape of power between specimen and flange. The specimen is thermally connected to the helium bath outside the can D only by means of the thin-walled copper-nickel tube E and copper tripod F. The tube E provides a well-defined

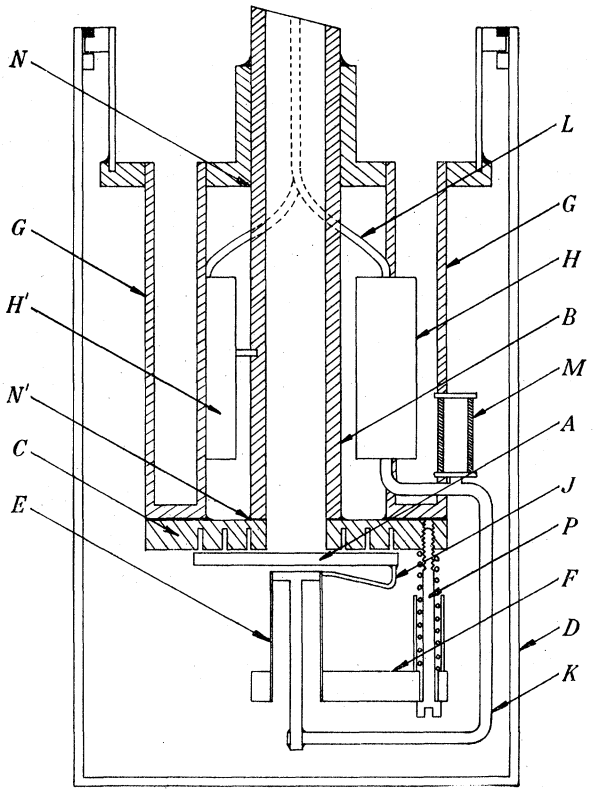

FIGURE 1. Schematic drawing of apparatus.

thermal resistance; otherwise there is good contact to the bath, since F is joined to C by a copper wire (not shown) and C is in direct contact with the bath through the two tubes GG. In order to achieve a well-defined bath temperature and therefore a well-defined temperature for C, all measurements were performed at a temperature of about 2·1° K, just below the λ point of helium, so that any heat generated in C was readily conducted away to the bath. Microwave power falling on A is largely reflected, but a small fraction is absorbed, proportional to the surface resistance of A. The temperature of A is thereby raised relative to the bath, and the difference in temperature is determined by means of a differential gas thermometer. One thermometer bulb, of 1 cm^3 capacity, is shown as H; it is in close thermal contact with the specimen through three copper wires J and the heavier copper wire K. The other bulb, not shown, is of the same size, but is maintained at the bath temperature by being attached to one of the tubes G. Thin-walled

copper-nickel tubes, as L, connect the thermometer bulbs to either side of a small differential oil manometer outside the cryostat. The bulbs were filled with helium gas at a pressure just less than the vapour pressure of the bath. In order to calibrate the system a heating coil M was attached near the bulb H; thus a given movement of the oil manometer could be easily related to the power absorbed in A without the need for any information about the gas law or dead space corrections.

It is also necessary to have a measure of the microwave power incident on the specimen, and for this purpose the waveguide B was made of brass, and its length and wall-thickness designed so that the temperature rise at its centre should be comparable with that of the specimen. To minimize variations of sensitivity with the microwave frequency it was arranged that N and N', the points of effective contact of the waveguide with the bath, should be as nearly as possible current nodes. The temperature rise at the centre was measured with the gas thermometer H', and as with the specimen thermometer there was a constant-temperature bulb (not shown), and a calibrating resistance coil was also attached to H'. It will be seen that the ratio of the energies absorbed in A and B is a measure of the surface resistance of A. We shall return later to the problem of calibrating the apparatus so as to derive absolute measures of the specimen resistance. In order to keep the thermal leaks well defined the whole apparatus must be kept in a high vacuum, by surrounding it by a can D. The pumping tube, by which it is evacuated to a pressure less than 10^{-6} mm Hg, is not shown. The electrical leads are taken from the cryostat through this tube.

Above the top of the can the brass rectangular waveguide B is bored out conically so as to mate with a circular copper-nickel waveguide, copper-plated on the inside. At the top of the cryostat a similar taper section returns the waveguide to rectangular form; this taper section also incorporates a mica disk and rubber ring as a vacuum seal. The transition to circular waveguide was made solely for the purpose of thermal isolation, since a thin-walled rectangular tube would not have withstood one atmosphere excess pressure outside. Previous experience had shown that this type of transition causes no difficulty, provided one avoids the narrow frequency bands within which the circular waveguide may resonate with a polarization perpendicular to that of the rectangular waveguides. The microwave power was supplied by a klystron; it was necessary to provide a tuning screw in the waveguide between klystron and cryostat in order to obtain any measurable output from the klystron into the highly resonant waveguide system. The power level at optimum tuning was equivalent to a flux of about 50 mW down the waveguide; of this about 5 μW was absorbed by the specimen and the rest reflected.

In order that the absorption of 5 μW should produce an accurately measurable movement of the specimen manometer, the thermal resistance of the tube E had to be made rather high, so that the time-constant for equilibrium of A was about 30 s. No hardship resulted from this, however, as the manometers showed only a very slight drift, and the klystron was quite stable enough to allow 4 min for A to come into equilibrium after switching the power on or off. The waveguide thermometer H', being in much closer contact with the bath, responded rapidly, and could be used as a monitor of the steadiness of the power input. With a power absorption of 5 μW the movement of one limb of the specimen manometer was about 4 mm. By observing the meniscus with a travelling

microscope this movement could be measured with an error of about $\pm 3 \times 10^{-3}$ mm, or less than 1 part in 1000.

Finally, let us return to the mounting of the specimen. In the first experiment the specimen was joined to the tube E by soldering the two directly together with tin-indium eutectic (m.p. 116° C). After the apparatus had been cooled to helium temperature and rewarmed it was found that the central region of the specimen was noticeably deformed, presumably as a result of differential contraction of the different parts. In all subsequent measurements, then, the specimen was supported by its edge on three copper wires J, soldered with tin-indium eutectic, and no damage resulted from this. The mounting of the specimen on the wires J was always carried out in a helium atmosphere. It may be mentioned here, and will arise again later, that the specimen damaged by differential contraction was ζ (table 1). X-ray examination showed the affected regions to be very small, and after repolishing it was used again, since no other crystal of this orientation was available. As will be seen, this has since proved to be a little unfortunate. The specimen after mounting on its holder was fixed in position opposite the flange C by means of three spring-loaded screws P. The spacing of A and C was about 0·2 mm, and was readily adjusted to be uniform by eye. Preliminary experiments showed that the exact spacing was of no significance, provided it was not too great, and in fact there was no difficulty in keeping within the safe range of variation suggested by these tests. The three screws P could fit into any of a ring of 12 holes in C, so that orientations of A in steps of 30° could be measured without separating A from J.

Accuracy of experimental results

The experimental method is liable to certain errors, and tests were made to estimate the importance of some of these, while others were minimized as far as possible in the conduct of the experiments. In the latter category may be placed variations resulting from different separations of the specimen from the flange C, already mentioned, and variations due to different frequencies being used for different specimens. This is believed to be only a small effect, and in any case care was taken to use as constant a frequency as possible, the total variation over all the experiments being from 22 685 to 22 710 Mc/s, or $\pm 0{\cdot}055$ %. The possibility of leakage of power past the chokes in C cannot be dismissed, especially in view of Fawcett's (1955) evidence that it occurred in his experiments. The effect of such leakage in causing spurious heating is not likely to be so important here as when carbon resistance thermometers are used, since the latter can pick up microwave power more readily than can gas thermometers. To examine this point a tin plate was used as specimen which, being superconducting, absorbed much less than a copper specimen. The absorption was found to be nearly the same for two different spacings between A and C, the wider being nearly 1 mm, and it was concluded that any error from this cause in the resistance of a copper specimen was unlikely to exceed 1 %.

It is more difficult to assess the errors resulting from variations in the surface quality of the specimen and from unsuspected random contributions connected with the mounting of the specimens. The experimental results tabulated in table 1 provide some evidence on this point. The specimen α, having a cube axis normal to its plane, should be isotropic, so that the four values of R given, two before and two after repolishing, should be identical.

Similarly ζ, having a (111) axis normal, should be isotropic; and the values of R_x and R_y for λ, while not identical, should be unaffected by repolishing. From an examination of this limited amount of data one may ascribe a r.m.s. error of 1·9 % to an individual reading. Further evidence may be obtained from measurements on the anisotropy of R in γ, which are shown in figure 2. The r.m.s. deviation from the theoretical straight line is 1·9 %, and it is thus probably safe to assume that the random errors in the experiments do not exceed 2 %. This is considerably greater than the apparent error of a single determination of R, for usually the ratio of deflexions of the two manometers was constant for repeated observations within 0·2 %.

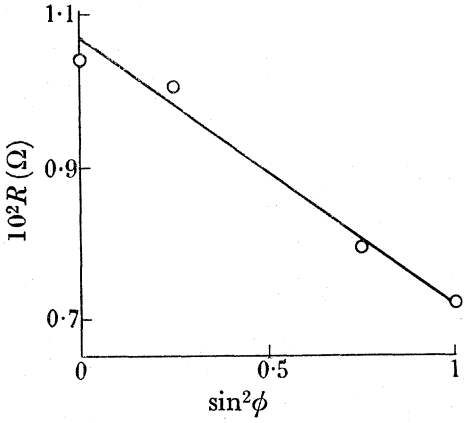

FIGURE 2. Variation with direction of current flow of resistance of specimen γ.

The apparatus was calibrated absolutely as in Fawcett's experiments, by the use of alloy specimens having sufficiently short electronic free paths that the skin resistance should be $2\pi\sqrt{(\nu\rho)}$, ν being the frequency and ρ the resistivity. Two specimens were used, one of α brass and the other of bronze. After the microwave measurements were completed, rectangular strips were cut from the specimens so that ρ could be determined. For the brass specimen, ρ at 4° K was $3{\cdot}71\times10^{-6}$ Ω cm, while for the bronze specimen it was $11{\cdot}26\times10^{-6}$ Ω cm. It would be expected from these values that the surface resistance of bronze would be 1·742 times that of brass. Three measurements were made on the brass specimen, at the beginning, middle and end of the series of measurements on the copper specimens. The values obtained for R, in arbitrary units, were 3437, 3209, 3290, giving a mean of 3312 with a r.m.s. deviation of 2·8 %. This is rather larger than the error estimated above, but probably not significantly so; at any rate there is no evidence of any serious drift in the performance of the apparatus with time. In the same units the resistance of bronze was 5740, so that the measured ratio of R is 1·733, in very good agreement with the predicted ratio. This supports the use of the formula $2\pi\sqrt{(\nu\rho)}$ for these alloys, and enables the arbitrary units of R to be converted into ohms. In view of the agreement obtained here it seems reasonable to hope that the absolute calibration of the apparatus is correct within about 2 %.

RESULTS

Twelve specimens of copper were used, having the crystal orientations shown in figure 3, which displays the orientations of the normals to the specimen surfaces on a stereographic plot. The specimens η to λ are displayed twice here in order to illustrate first, that the

orientations of the specimens map out the bounds of the spherical triangle defined by the (100), (110) and (111) axes which is sufficient, with the symmetry properties of a cubic crystal, to define the behaviour in any direction; and secondly, that the series from α to λ form a continuous series in which the crystal may be imagined rotated about a (110) axis lying in the plane of the surface of the specimen, so that the (100) axis originally normal to the plane in α is eventually lying in the plane in λ. In table 1 this series is referred to as series 1, and the angle θ is the angle between the normal to the surface and the appropriate (100) axis, as illustrated schematically in figure 4 (a). Series 2 starts with the orientation α and rotates about a (100) axis lying in the surface of the specimen, as illustrated in figure 4 (b); for this series, of course, θ and $90° - \theta$ are equivalent orientations.

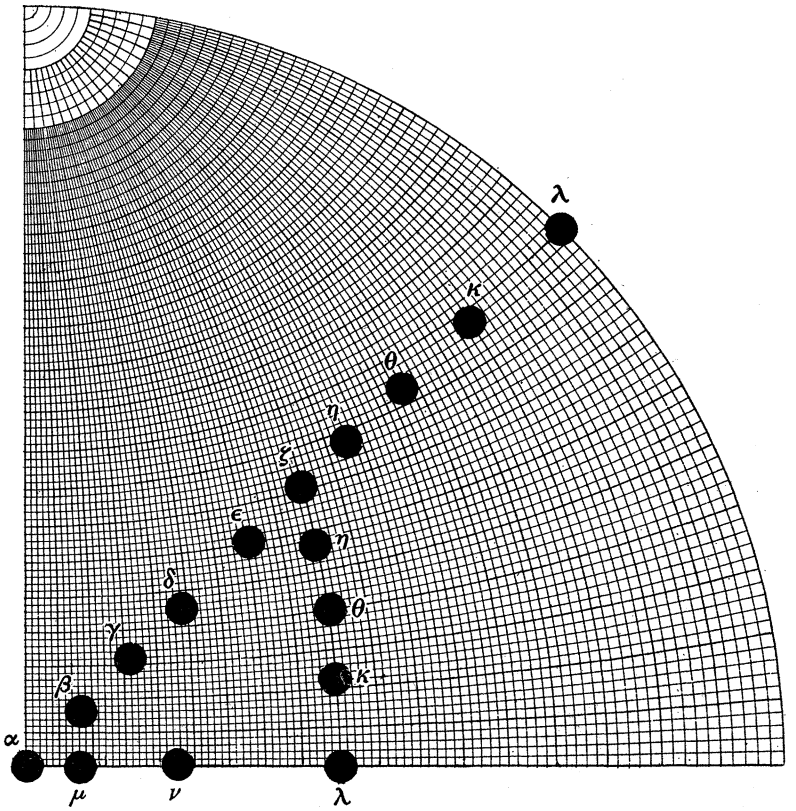

FIGURE 3. Stereographic chart of normals to the surfaces of the specimens; α is (100), ζ (111) and λ (110).

The two diagrams in each of figures 4 (a) and (b) show the directions of current flow which yielded the resistances R_x and R_y given in table 1 and plotted in figure 5. There is no doubt for any of the orientations used which are the principal axes of the surface resistance tensor; for any orientation not lying on a plane of crystal symmetry the principal axes could only be determined by experiment. It may be remarked in passing that the sectioning of the cubes in figures 4 (a) and 4 (b) illustrates the problem involved in computing R_x and R_y from equations (2) and (3). In each plane section the effective zone must be located as the point where the normal to the surface lies parallel to the xy plane, and the radius of curvature in the section determined at this point. The integrals in (2) and (3) are then represented as the summation over all the sections.

To return to figure 5, it will be observed that while R_x and R_y for series 2 and R_y for series 1 all show a smooth variation, the variation of R_x in series 1 is much more complex. It might indeed be doubted whether there are sufficient experimental points to justify drawing a smooth curve, since the discovery of a serious error in almost any one point

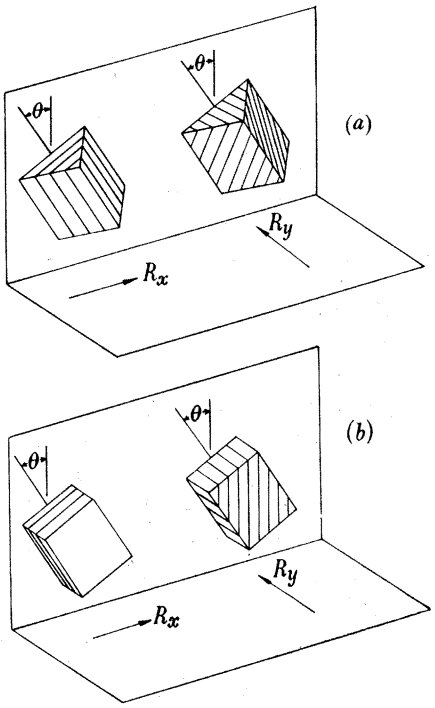

FIGURE 4. Schematic representation of orientations in (*a*) series 1, (*b*) series 2.

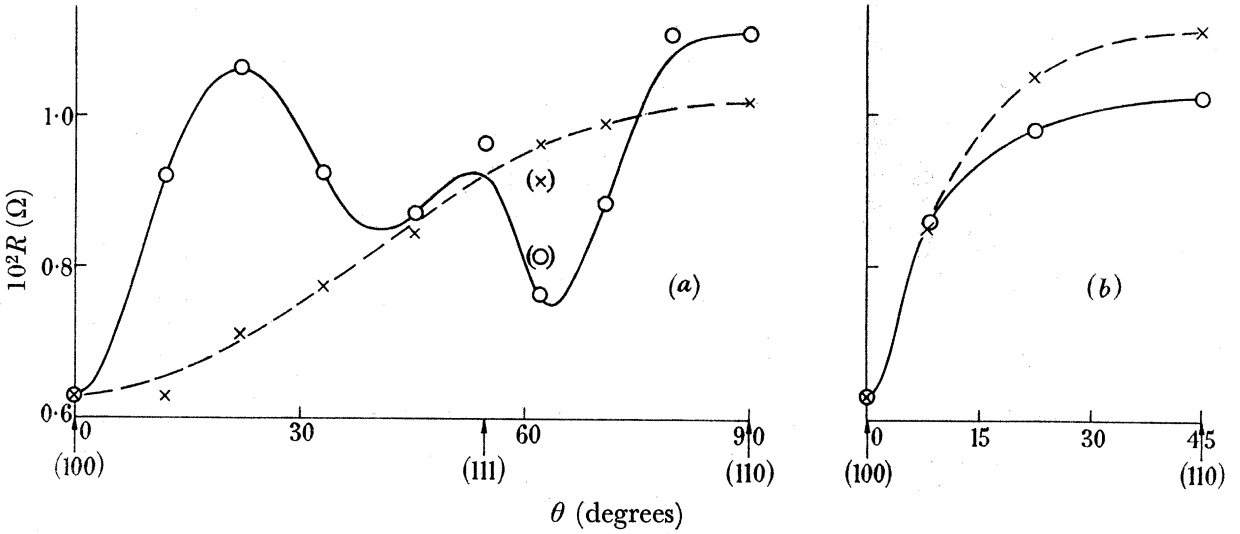

FIGURE 5. Experimental results: (*a*) series 1, (*b*) series 2; ○, R_x; ×, R_y; the points in brackets are the actual measurements for η (see note in table 1).

would be sufficient to cast doubt on the general shape. The smoothness of the points for R_y in series 1, however, seems sufficient justification for presuming good surface preparation of the specimens, and of all the points on the R_y curve only that for specimen ζ gives the impression of considerable error. This specimen indeed is the one which was damaged

in the first experiment, as already described, and is the only one for which there exists an obvious explanation for a discrepancy. It is therefore more a matter for regret than surprise to ignore it in drawing a smooth curve for R_y. And because this specimen has a (111) axis normal to its plane, it must be isotropic in its surface resistance, so that the curve for R_x is automatically drawn through this point. There is a further unfortunate doubt about the points for the neighbouring specimen η, owing to a crystallographic error not discovered until too late, so that the resistance was measured along directions inclined at 30° to the principal directions. The actual measurements are shown in brackets in figure 5, from which it is clear that correction of the value of R_y is a very plausible improvement, while correction of R_x enhances rather than creates the deep dip in the curve.

Apart from these points of doubt, there is no evidence from the experiments themselves to suggest that any of the other results should be neglected in constructing the curves, and we shall therefore trust to the estimated probable error of 2% and assume that within this limit of accuracy the curves drawn in figure 5 are indeed a true representation of the anisotropy of the surface resistance, for which an explanation must be found in terms of the shape of the Fermi surface.*

Construction of the Fermi surface

According to (2) and (3) the surface resistance is determined by integrals of the radius of curvature of sections of the Fermi surface, taken around the effective zone or zones, and in particular $R \propto \mathscr{I}^{-\frac{1}{3}}$ where $\mathscr{I}$ is an integral of the type $\int |\rho_y| \, dy$. It is clear then that since the extreme values of R differ by a factor 1·77, the extreme values of $\mathscr{I}$ differ by a factor 5·5, and the local curvatures probably vary over a greater range than this. We may therefore expect considerable departures of the Fermi surface from spherical form. It should be remembered, however, that it is quite possible to deform a sphere into a surface having a large number of flat areas without any great changes in the radius vector, and such a deformed sphere will show wide variations in $\mathscr{I}$ as more or less flat regions lie on the effective zone.

Although in constructing a surface having the required variations of curvature we shall make as little use as possible of physical ideas, in order to avoid bias through preconceived notions, it will be as well to consider at the outset whether we may reasonably expect the Fermi surface in copper to consist of a single sheet. Certainly the majority of the conduction electrons must be derived from the set of wave functions for the single valence electron of the free atom, and we may expect the lowest energy in the valence band to lie at the centre of the Brillouin zone. If this band were isotropic the Fermi sphere, containing one electron per atom, would lie comfortably within the truncated octahedral zone, the nearest boundary being at a distance from the centre 1·10803 times the radius of the sphere. The contingencies which could conceivably give rise to multiple Fermi surfaces are, first, that the 3d shell is not completely filled, so that there is a set of small holes, and a valence

* It may perhaps be said in explanation of the small number of experimental points and the doubts about the validity of a few of these, that the experiments were performed under the restrictions of a time limit at the University of Chicago, and that it was only owing to the generosity of the University in removing all other restrictions that the work reached even this stage of completion.

PHILOSOPHICAL TRANSACTIONS OF THE ROYAL SOCIETY A MATHEMATICAL, PHYSICAL & ENGINEERING SCIENCES

band containing more than one electron per atom, and, secondly, that the valence band not only touches the Brillouin zone but overlaps into higher zones. Both these types of behaviour tend to increase the total area of the Fermi surfaces over the value for a sphere containing one electron per atom, and it is noteworthy that Chambers (1952) in his study of the anomalous skin effect of polycrystalline copper, concluded that the total area was very close indeed to that of the ideal sphere. This conclusion, as will be seen in due course, is substantiated by the present results. It may also be argued against the lack of completeness of the 3*d* shell, that the positive holes would give rise to a de Haas–van Alphen effect in low magnetic fields, and this has not been observed. But such arguments and arguments based on alloy behaviour, although pointing in the same direction, are not so incontrovertible as to be used except to bolster up the belief, based on Chambers's result, that a single Fermi surface of cubic symmetry is a good starting hypothesis. We may supplement this hypothesis by a second, more tentative, assumption that the Fermi surface is nearly everywhere convex.

Some qualitative features of figure 5 provide useful hints as to the shape of surface to be considered. In series 1 the irregularity of R_x contrasts strongly with the smoothness of R_y; it may also be observed that the resistance along a cube axis is as low as any orientation when another cube axis is normal to the specimen ($\theta = 0$ in series 1), but that rotation through 45° so that a (110) axis is normal to the specimen ($\theta = 90°$ in series 1) raises the resistance along a cube axis to the highest value observed. This latter feature shows that the major contribution to $\mathscr{I}$ does not come from a flattening around the (100) position on the Fermi surface, since ρ must be isotropic at this point (it will be taken for granted that if the Fermi surface is closed it is free from singularities). If now we take up the first feature remarked on, we may understand the contrast between R_x and R_y in series 1 by supposing that there is one region of the Fermi surface which dominates the behaviour of R_y, and whose curvature in the appropriate section is a smooth function of θ, while R_x is dominated by different regions which pass through the effective zone as θ is changed. Now the only part of the surface which remains effective for all values of θ, and which can therefore satisfy the requirement of always dominating R_y, is in the (110) position, where the normal to the Fermi surface is the axis about which the crystal is rotated in series 1. We may therefore look for a surface which is rather sharply creased at the (110) positions, so that in a plane normal to a (110) axis the radius of curvature is large, while in a plane normal to a (100) axis it is small. A cube is an extreme example of such a surface, but the cube will not serve as a model for the Fermi surface since it is flattened on the (100) axes. A closer approximation to the type of surface required is the curvilinear dodecahedron formed by the intersection of three mutually perpendicular cylinders; this is shown in figure 6, the ends of typical (100), (110) and (111) axes being labelled *X*, *K* and *L*, respectively. It will be observed that the requirements of a large radius of curvature along *KL* pushes out the surface at *L*. This then makes possible, by slight adjustment of the shape, a rather flat region between *X* and *L* which can account for the sharp drop in R_x of series 1 around 65°.

This general argument makes it likely that the type of surface of which figure 6 is an extreme example can be made to account satisfactorily for the experimental results, and indeed it is hard to see that any other type of closed surface will fit the facts. With this in

mind an analytical approach to the problem was undertaken, starting with a surface of the form

$$x^2+y^2+z^2-ax^2y^2z^2+b\,(x^2y^2+y^2z^2+z^2x^2)=1. \tag{4}$$

Roughly, the effect of the term $ax^2y^2z^2$ is to modify a sphere by extension at the points L, while the term $b\,(x^2y^2+y^2z^2+z^2x^2)$ depresses the points K, and thus enhances the

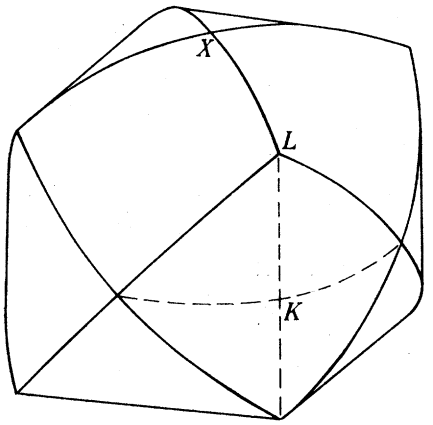

FIGURE 6. Curvilinear dodecahedron.

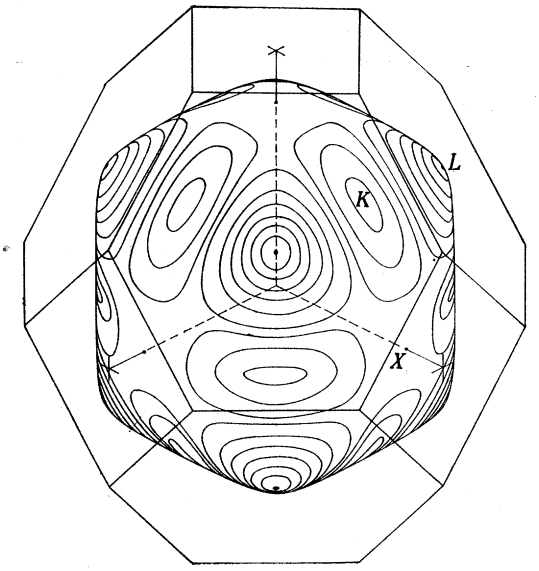

FIGURE 7. Surface satisfying equation (4) with $a=5{\cdot}6$, $b=0{\cdot}3$, enclosed in Brillouin zone for copper. Contours of constant radius vector are drawn on the surface. The intersections of the cube axes with the Brillouin zone are indicated by crosses. [*Note added in proof:* by a constructional error this diagram and figure 18 also are distorted, the vertical scale being about 10% too large in comparison with the horizontal scale.]

ridges joining XL. A typical surface of this type is drawn in figure 7, for which $a=5{\cdot}6$ and $b=0{\cdot}3$; the lines are contours of constant radius vector. The surface represented by (4) is closed only for values of a and b within the restricted range

$$a\leqslant\frac{2-3\alpha}{\alpha^3},\quad \text{where } \alpha=\frac{\sqrt{(1+b)}-1}{b}. \tag{5}$$

Thus the surface shown in figure 7 is rather near to a critical surface, since when $b=0{\cdot}3$ the value of a must be less than 5·865. When the critical values of a and b are reached the

surface becomes pointed at L, and the curvature at K becomes zero in the plane containing KL; near, but not necessarily at, the critical condition a region of zero curvature develops also on the ridge XL.

There are two particularly symmetrical crystal orientations for which the effective zone lies in the plane of the specimen, and the integrals $\mathscr{I}$ can be computed with little labour. These directions correspond to values for θ of 0 and 90° in series 1, and thus three separate values of R are readily computed from (4), i.e. R_x (0), R_x (90°) and R_y (90°) in series 1. As a first attempt to find a surface which would account for all the observations, values of a (=6·6) and b (=0·5) were chosen so that the relative values of these three resistances were given correctly. The curve for R_x in series 1 was then computed in the following way. The equation of the surface was first referred to axes rotated through 45° about the z axis, normal to the specimen:

$$z^2 = \frac{(1-y^2-\frac{1}{4}by^4)-(1-\frac{1}{2}by^2)x^2-\frac{1}{4}bx^4}{(1+by^2-\frac{1}{4}ay^4)+(b+\frac{1}{2}ay^2)x^2-\frac{1}{4}ax^4}. \tag{6}$$

From this equation tables were constructed on the digital computer EDSAC, showing $(\partial z/\partial x)_y$ and $\rho_y[=\{1+(\partial z/\partial x)_y^2\}^{\frac{3}{2}}/(\partial^2 z/\partial x^2)_y]$ as functions of x, for a series of sections $y=$ constant. For any particular crystal orientation θ in series 1, the effective zone in each section is discovered in the tables as that point where $(\partial z/\partial x)_y=\cot\theta$. The corresponding value of ρ_y may then be plotted as a function of y, and the integral $\int|\rho_y|\,\mathrm{d}y$ evaluated. Since what is needed for comparison with experiment is the cube root of the integral, it is not hard to achieve adequate accuracy in the numerical work.

The behaviour of this first trial surface was encouraging, the general shape of the R_x curve being well reproduced, except that instead of a minimum at 40° and a maximum at 53° there was only a slight inflexion in the curve as it fell from its peak at 20° to its deep trough at 64°; it was significant also that at 54·7°, where the required value of R_x is rather closely specified by the smooth curve for R_y, the predicted value was about 15% too low. It was verified rather roughly that the behaviour of R_y is indeed smooth for this trial surface, and the predicted values of R_y are all too low in this central region of series 1.

If better agreement is to be obtained in this central region, different parameters a and b must be chosen, and the agreement at the extremes must then be abandoned. Alternatively, the model surface given by (4) must be made more general by the addition of further terms, or the shape must be adjusted by graphical methods, both of which alternatives offer a considerable increase in complication. It was realized, however, that close agreement at the extremes was neither necessary, nor indeed desirable, particularly as regards the low value when $\theta=0$, for the theory contains an approximation which assumes some importance for surfaces having regions of very small curvature. The radius of curvature on the effective zone enters into the theory as defining the extent of that region of the Fermi surface for which the electrons are moving nearly parallel to the surface of the specimen. In the intuitive form of the theory given in I, and fairly thoroughly justified by Kaganov & Azbel′ (1955), the effective electrons are taken to be those whose motions are inclined to the surface at an angle less than $\beta\delta_r/l$, in which β is a numerical constant $8\pi/3^{\frac{3}{2}}$, δ_r is the resistive skin depth defined as $R/(2\pi\omega)$ (R being measured in e.m.u.) and l is the

electronic mean free path. It is only when ρ is sensibly constant over this angular range that the expressions (2) and (3) strictly apply. Now if we take as a reasonable average $0{\cdot}0087\,\Omega$ as the value of R and Chambers's (1952) value for σ/l, we find that for copper having a residual resistance 200 times less than the room-temperature value the angle within which the electrons must move to be effective is $\pm 3{\cdot}7°$. It will now be seen from figure 8 that where the value of ρ is high, and the contribution to the integral $\mathscr{I}$ greatest, ρ is far from constant over a range of $7{\cdot}4°$.

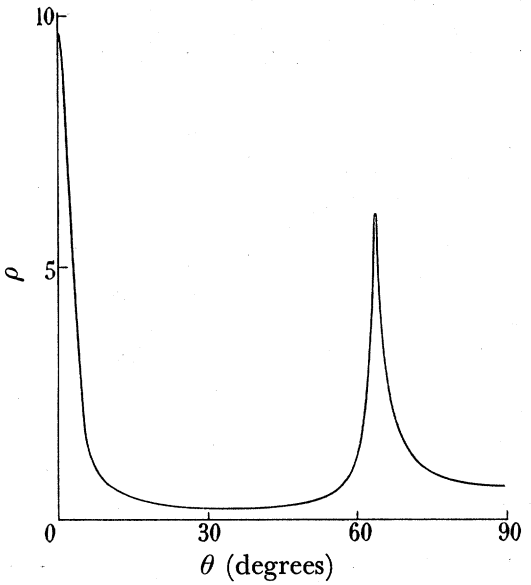

FIGURE 8. Variation of radius of curvature with inclination of normal for central section of first trial surface.

A plausible way of allowing for the variation of ρ is to replace $|\rho|$ in $\mathscr{I}$ by $\overline{|\rho|}$, the average of $|\rho|$ over the appropriate angular range. It has not been demonstrated that this is the correct procedure, but it is in keeping with the spirit of the ineffectiveness concept which was used in I to derive the forms for R_x and R_y (equations (2) and (3)) which are believed to be correct. In essence one replaces the actual Fermi surface by an equivalent spherical surface, having a curvature around the effective zone which is dependent on the free path. This means that for an orientation where the curvature changes rapidly, the approach of the resistance to its limiting value (as $l \to \infty$) should not follow the law deduced by Reuter & Sondheimer (1948) for a spherical Fermi surface. The problems which this raises are not of great importance, however, and we shall not discuss them at this point. What is of more immediate interest is that the low value of R when $\theta = 0$ in series 1 is not to be immediately related to equation (2), so that if we leave this point aside for the present we are at liberty to consider different values of the parameters a and b in order to get a better general fit to the experimental points.

Further calculation soon made it clear that to maintain a fit to the values in series 1 at 90° and to raise the value at $54{\cdot}7°$ required a closer approach to critical values of a and b than was attempted in the first trial surface, and a was now taken as $5{\cdot}6$, b as $0{\cdot}3$; this is the surface drawn in figure 7. The computed variation for series 1 of $\mathscr{I}_x^{-\frac{1}{3}}$, which is proportional to R_x, is shown in figure 9, together with the experimental points suitably

scaled. The point at 54·7° is that deduced from the smooth variation of R_y, not the dubious experimental point. Some idea of the effect of the rapid variation of ρ is given by the broken curve near 0°, which is computed by taking average values of ρ over a range of $\pm 3{\cdot}7°$. The correction applied here is too large, since R and ρ are particularly small here, and the angle in which the effective electrons move is rather smaller than the average. No correction has been computed for the curve around 65°. The deviations of the experimental points from the computed curve are now less than 7 %, which is still considerably more than the estimated error. The discrepancy at 54·7° has been reduced to 6 % by the new choice of parameters, but there is still no sign of the desired dip around 40°.

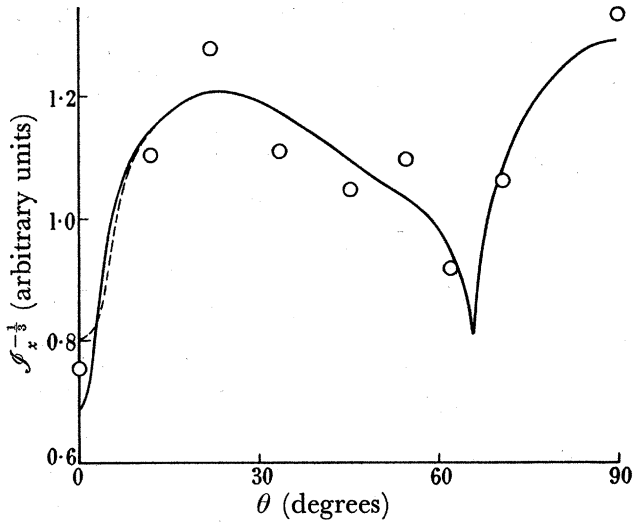

FIGURE 9. Computed variation of $\mathscr{S}_x^{-\frac{1}{3}}$ with θ for series 1, using trial surface with $a = 5{\cdot}6$, $b = 0{\cdot}3$. The broken curve shows the effect of averaging ρ over the effective angular range.

At this stage it was decided that little hope of improvement lay in further adjustment of the parameters, and that graphical methods must be employed to construct an improved surface. It was suggested in I that the analysis of the experimental data might prove extremely tedious, and this foreboding was now found to be amply confirmed. This matter is worth remarking on since the difficulty of handling the data must play a part when we come to assess the usefulness of the method. Great delicacy is required in applying small corrections to the analytical form of the surface by graphical means, since the radius of curvature may be considerably altered by a very small change of radius vector, and errors in the estimated values of ρ easily assume significant proportions unless the greatest of care is taken in drawing. The method used is described in an appendix.

It was first noted by Chambers (1952) that the average value of R for all crystal orientations is determined by the total area of the Fermi surface. This result makes it clear that any small adjustment of the shape of the Fermi surface which is sufficient to modify R for one orientation is liable to produce an opposite change in R for another orientation, since the area of the Fermi surface is little affected by these small adjustments. With perseverance, then, one may hope to rectify most, if not all, of the discrepancies in figure 9 by an appropriate choice of correction. After some trial and error the correction shown in the stereographic plot of figure 10 was studied in detail. Only one-sixteenth of the total solid

angle is shown here, but the corrections in other directions are easily obtained by the appropriate symmetry operations. The contours show, as a function of direction of the radius vector, corrections which are to be subtracted from the radius vector. The greatest correction only amounts to 0·8 % change of radius, but this is sufficient to produce a slight concavity in the ridge XL, and to cause considerable modification to the form of the curve

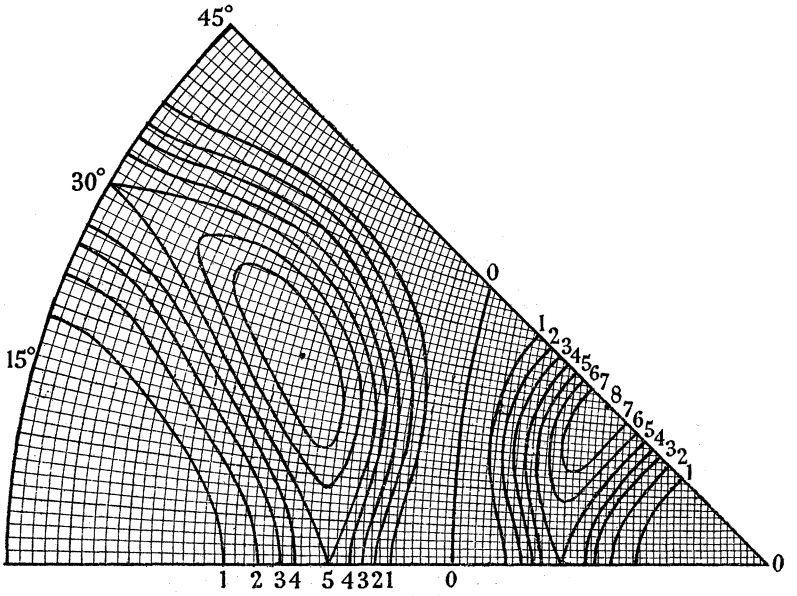

FIGURE 10. Graphical correction to trial surface with $a = 5{\cdot}6$, $b = 0{\cdot}3$. The figures labelling the contours represent 1000 times the correction to be subtracted from the radius vector.

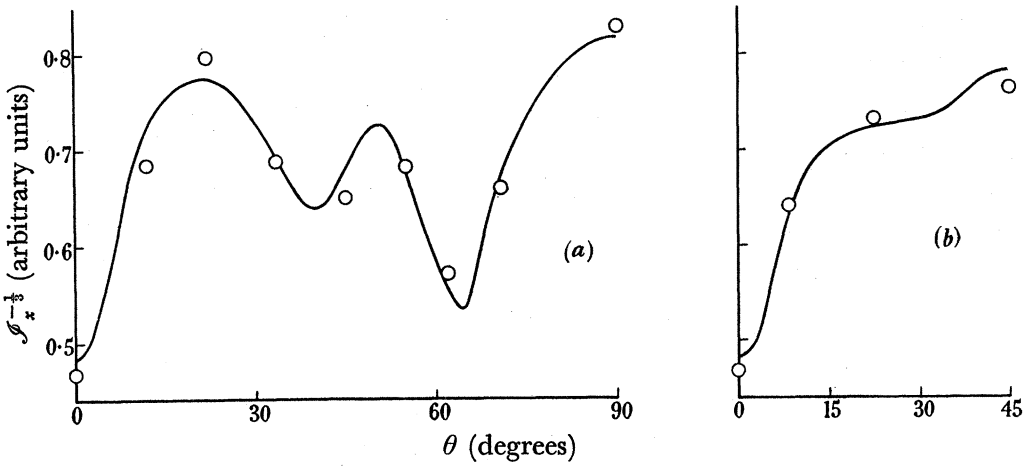

FIGURE 11. Computed variation of $\mathscr{I}_x^{-\frac{1}{3}}$ with θ for corrected surface, compared with scaled experimental points: (*a*) series 1, (*b*) series 2.

for R. The appearance of concavities makes it essential to average the radius of curvature over the appropriate effective angle, and this averaging has been done in computing the curves shown in figure 11. The same computations of R_x were carried out for the orientations comprising series 2 in table 1, and these are also shown in figure 11. Clearly, the graphical adjustment of the surface has improved the agreement. After scaling the experimental points to give the best fits to the two curves for R_x, the greatest deviation is

4·3 % and the r.m.s. deviation of all points is 2·7 %. This is slightly larger than the estimated experimental error of 2 %, but it must be remembered that this estimate was based on very little information, and in addition the computed curves may well be somewhat in error owing to the graphical method used. It was thought, in view of this measure of agreement, that the experimental information did not warrant any further attempts to adjust the Fermi surface.

It will be noted that virtually no attempt has been made to use the data for R_y in any quantitative way, except to fix the value of R_x at 54·7° in series 1. This is because the procedure involved in computing a theoretical curve for R_y is, even with an analytic form of surface, much more elaborate than for R_x, and, when graphical adjustments are brought in, not only exceedingly laborious but of dubious accuracy. It was, however, verified by a few calculations that with an analytical surface of the type (4), R_y in series 1 is a smooth curve as expected, since it is dominated by the highly anisotropic curvature of the surface at K; it is believed that the graphical correction will not seriously disturb the smoothness of this curve.

The conclusion of this analysis is then that the experimental points are explained by a Fermi surface obeying equation (4), with $a=5{\cdot}6$ and $b=0{\cdot}3$, modified by subtracting the small corrections shown as contours in figure 10. The appearance of this surface is hardly distinguishable from that shown in figure 7, the salient features being the extensions in the (111) directions at such points as L, the anisotropic curvature at such points as K, with almost zero curvature in the direction KL, and the rudimentary ridge along XL, with a saddle point where the curvature along XL becomes very slightly concave.

Absolute magnitude of the surface resistance

So far we have been content to find a shape of Fermi surface which will reproduce the relative values of R in different orientations. It is now necessary to examine the absolute magnitude of R and of the Fermi surface, to see whether the interpretation of the measurements is consistent with the generally accepted properties of copper. What we shall do is to determine the volume of the Fermi surface as given by (4) with the corrections already described, and hence discover what is the scale factor required to convert it into a figure which will hold one electron per atom in copper. This will immediately fix the absolute magnitude of the radii of curvature and of the integrals $\mathscr{I}$, so that absolute values of R may be predicted for all orientations.

The volume of the Fermi surface is best computed in stages, beginning with the uncorrected surface (4). Sections normal to a cube axis have areas that may be expressed in terms of tabulated or easily calculated elliptic integrals, and these areas do not differ greatly from the areas of corresponding sections of a unit sphere. Thus the difference between the actual volume and that of a unit sphere is readily found with adequate accuracy by a single graphical integration. The change in volume due to the correction shown in figure 10 amounted to less than 1%, and was estimated graphically. The result of this calculation is that the volume of the Fermi surface is 4·176, with an estimated error of 1/20 %; this may be compared with the volume of a unit sphere, 4·189.

If the density of copper at 0° K be taken as 9·027 g cm^{-3}, then there are $8{\cdot}557\times10^{22}$ conduction electrons per cubic centimetre, allowing one per atom, and these must occupy a

volume in momentum space of $8{\cdot}557 \times 10^{22}\, h^3/2$. If the unit of length in our previous computations is to be interpreted as P_0 g cm s^{-1}, we may equate the volume of the Fermi surface to the volume required to hold one electron per atom, and deduce that $P_0 = 1{\cdot}439 \times 10^{-19}$ g cm s^{-1}, the momentum of a free electron of 7·10 eV energy. When the values of the parameters are inserted in (2) it is found that the factor needed to convert values of $\mathscr{I}^{-\frac{1}{3}}$ into values of R in ohms is $1{\cdot}3145 \times 10^{-2}$. It is a comparison of this figure with what is required to fit the experimental points to the curves of figure 11 which tests the validity of two assumptions, that the theory of the anomalous skin effect, leading to (2) and (3), is correct, and that the Fermi surface in copper contains one electron per atom.

TABLE 2

specimen		$\mathscr{I}^{-\frac{1}{3}}$	$10^2 R_{\text{theor.}}(\Omega)$	$10^2 R_{\text{meas.}}(\Omega)$	$R_{\text{theor.}}/R_{\text{meas.}}$
series 1	α	0·482	0·643	0·629	1·022
	β	0·720	0·960	0·920	1·043
	γ	0·776	1·035	1·065	0·972
	δ	0·696	0·928	0·925	1·003
	ϵ	0·683	0·911	0·873	1·044
	η	0·554	0·739	0·765	0·966
	θ	0·675	0·900	0·885	1·017
	λ	0·816	1·089	1·110	0·981
series 2	μ	0·630	0·840	0·859	0·978
	ν	0·724	0·966	0·981	0·985
	λ	0·781	1·042	1·022	1·020
					1·003 (mean)
					r.m.s. deviation = 0·027

But before the comparison is to be made, some further small adjustments are necessary. The theory derived expressions for the surface resistance in the limit of infinite free path, on the assumption that relaxation effects are negligible. The latter are a result of the finite electronic velocity, and lead to a decrease of the measured resistance below the theoretical value without relaxation. Tables have been compiled by Dingle (1953) and Chambers (1953) which enable the correction to be estimated, when reasonable values of the parameters are introduced, as 3·7 %. The effect of finite free path is to increase the measured resistance above the theoretical limiting value, to the extent of 5·2 % as computed from Reuter & Sondheimer's (1948) theory. Both these corrections are intended as averages over all crystal orientations; to find how they varied with orientation would require detailed knowledge of the variation of free path and electronic velocity over the Fermi surface. The resultant correction of 1·5 % should therefore be regarded as liable to variations probably as large as itself, but it is probably not so uncertain when taken as a mean correction. With this correction we may state the expected factor to convert calculated values of $\mathscr{I}^{-\frac{1}{3}}$ into measured values of R to be $1{\cdot}334 \times 10^{-2}$. A detailed comparison between theory and experiment is shown in table 2, the agreement being well within the limits of error due to experiment and computation. Thus there is no reason to doubt the quantitative validity of the theory, nor the assumption that only the valence electrons in copper contribute to electrical conduction. It will be noted that there is here no sign of the systematic discrepancy found by Fawcett (1955), whose values for the resistance of several metals, including copper, at 36000 Mc/s appeared to be up to 12 % too high.

PHILOSOPHICAL TRANSACTIONS OF THE ROYAL SOCIETY A MATHEMATICAL, PHYSICAL & ENGINEERING SCIENCES

The Fermi surface and Brillouin zone

The Fermi surface has been constructed without any consideration being given to the way it has to be contained within the Brillouin zone, which is a truncated octahedron capable of holding two electrons per atom, as shown in figure 12. In figure 7 is another aspect of the Brillouin zone, which shows its relation to the Fermi surface. As might have been expected, the greatest extensions of the Fermi surface occur at L opposite the centres of the hexagonal faces, which are the points nearest the centre of the zone. If we continue to use the units in which (4) and the correction contours of figure 10 are expressed, the volume of the zone must be 8·352, and this means that ΓL is 1·1069, and ΓX, the radius to the centres of the squares, is 1·2781. The radii in these directions of the Fermi surface which we have devised are 1·1162 and 1·0000, respectively. Thus the surface fails by 0·8 % of its

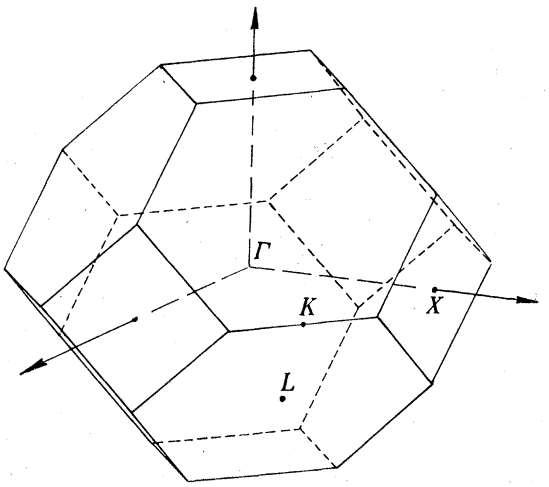

Figure 12. Brillouin zone for copper.

radius vector to fit into the Brillouin zone at the centres of the hexagons. This makes it imperative to examine the shape of the surface in the neighbourhood of L to see whether it can be modified so as to fit into the zone without destroying agreement between theoretical and experimental values of R. It should be clear from the changes resulting from applying the corrections of figure 10 that no considerable alteration in shape can be contemplated.

The problem is exhibited in figure 13, which shows a quadrant of the Fermi surface in a central plane ΓKLX (figure 12), together with sections of the zone boundaries. The question to be decided is whether the overlap at L is to be eliminated by pushing the Fermi surface into the zone (as shown by the dotted line) or by allowing contact with the boundary (roughly as shown by the broken lines). To make either change is liable to upset the predicted form of the resistance curves, but not seriously so long as the change is confined to a small area around L, where the curvature is in any case high and the contribution to conductivity small. A decision between the alternatives involves recourse to physical arguments in order to discover what is the likely shape of an energy surface near the zone boundary.

It may be seen at once that whatever the final solution it is probable that the Fermi surface will run extremely close to the zone boundary at L, so that the shape must be very nearly that of the critical energy surface which just makes contact at L. Since in the vicinity

of a zone boundary the effective mass approximation is good, it is to be expected that the surfaces of nearly critical energy will be hyperboloids of revolution about an axis normal to the boundary at L, having as an asymptotic surface a cone whose apex is L, such as is shown diagrammatically in figure 14. If ψ is the semi-angle of the cone, and m_t and m_n the effective masses tangential and normal to the boundary, then $\tan\psi = (m_t/m_n)^{\frac{1}{2}}$. The effective mass approximation breaks down not far from L, and we shall consider improved forms of energy surfaces later. It will be observed from figure 13 that the Fermi surface

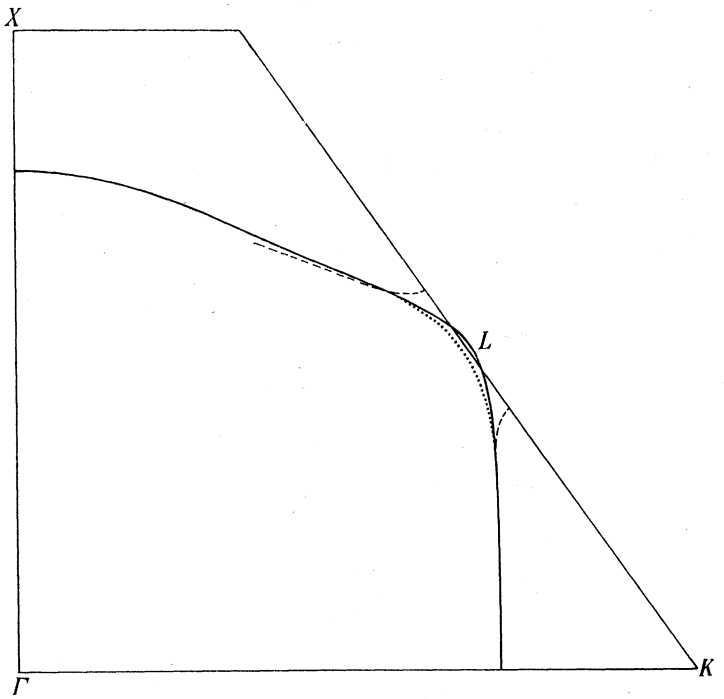

FIGURE 13. Section of zone and corrected surface, showing overlap at L. The broken curve is computed from the Kronig–Penney model (see text), and the dotted curve is a suggested modification to the surface to avoid contact or overlap.

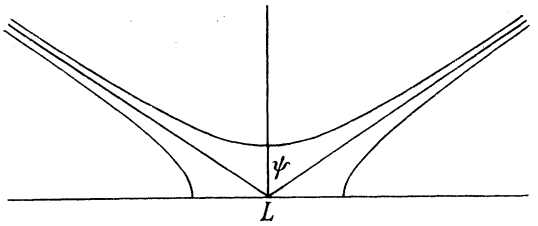

FIGURE 14. Theoretical sections of constant energy surfaces near contact with zone boundary.

arrived at from the experimental results has this in common with the theoretical prediction, that in the vicinity of L it is very nearly a surface of revolution about the normal. Moreover, the fact that the radius in the plane of the section bccomes very large such a short distance from L accords with the idea that it lies very close to the critical energy surface.

In order to see which of the alternatives is the more probable, some model is needed to provide the relation between energy and momentum normal to the zone boundary. If the asymptotic surface is to follow the derived Fermi surface except very close to L the

effective mass ratio m_t/m_n must be about 4. Such a value implies an energy gap across the zone boundary which is comparable with the kinetic energy of an electron at L, and neither the almost-free nor the tight-binding approximations are really suitable to describe this situation. We shall therefore take as a model the one-dimensional model of Kronig & Penney (1930), which has the merit of being amenable to exact calculation under all circumstances. The general form of the model is shown in figure 15 (a), but for convenience the δ function model of 15 (b) will be used. Even when the energy gap at the first zone boundary is comparable with the kinetic energy it appears by direct calculation that the energy-momentum relation does not depend to any significant degree on the form of the potential, being determined solely by the energy gap; the results derived from the δ function model are thus probably valid for almost any one-dimensional periodic potential function. It would be too much to hope that they would also be valid for a three-dimensional metal, but in the absence of any simple treatment of a more realistic model we shall assume that the one-dimensional model gives the correct result, bearing in mind that only moderate faith should be placed in this assumption.

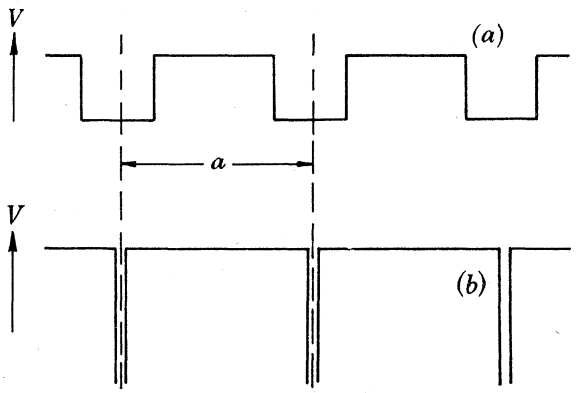

FIGURE 15. Kronig–Penney one-dimensional periodic potential: (a) general, (b) δ function model.

The essential results of the δ function model may be stated as follows. Let the momentum (i.e. $\hbar k$) of the electron in the lattice be represented by $\hbar\alpha/a$, so that at the zone boundary, where $k=\pi/a$, $\alpha=\pi$; let the energy of the electron be represented by ϕ^2, the unit of mass being chosen so that for a free electron $\phi=\alpha$; then

$$\cos\alpha = \cos\phi - C\sin\phi/\phi, \tag{7}$$

in which C is a measure of the negative area of the δ function in figure 15 (b). A typical graph of ϕ^2 against α, i.e. energy against momentum, is shown in figure 16, for $C=1{\cdot}80$. At the bottom of the band the curve is parabolic, and the effective mass, relative to a free electron, is given by the expression

$$(m_{\text{eff.}})_0 = \frac{C}{\mu_0^2}\left(1+\frac{\sinh\mu_0}{\mu_0}\right), \tag{8}$$

where μ_0 is the solution of the equation $C=\mu_0\tanh(\frac{1}{2}\mu_0)$. At the top of the band the effective mass is given by the expression

$$(m_{\text{eff.}})_\pi = \frac{C}{\phi_\pi^2}\left(1-\frac{\sin\phi_\pi}{\phi_\pi}\right), \tag{9}$$

where ϕ_π is the solution of the equation $C=\phi_\pi \cot(\frac{1}{2}\phi_\pi)$. The band width is $\phi_\pi^2+\mu_0^2$, and the energy gap above the band is $\pi^2-\phi_\pi^2$.

We shall now assume that these expressions describe the variation of energy along the normal to the zone boundary, i.e. along ΓL in figure 13, so that m_n is put equal to $(m_{\text{eff.}})_\pi$. We shall further assume that the increment of energy associated with movement normal to ΓL is independent of the position along ΓL; since therefore $m_{\text{eff.}}$ is isotropic at the origin Γ, we take m_t to be equal to $(m_{\text{eff.}})_0$, and we suppose that the parabolic approximation holds to considerable distances from ΓL. It is now easy to calculate the shapes of constant-energy surfaces near L, for any given value of C. The broken line in figure 13 is such a surface with C equal to 1·80; for this value $(m_{\text{eff.}})_0 = 1{\cdot}1066$ and $(m_{\text{eff.}})_\pi = 0{\cdot}2828$, the band width, $\phi_\pi^2+\mu_0^2$, i.e. the kinetic energy of an electron on the asymptotic surface, is 6·16, and the energy gap at L, $\pi^2-\phi_\pi^2$, is 8·69. The surface drawn in figure 13 corresponds to a kinetic energy of 6·31, slightly higher than that of the asymptote. These energies are given in the units of this section of which one unit is equal to 0·8808 eV; in electron volts the kinetic energy at the Fermi surface is 5·56 eV, and the energy gap at L is 7·65 eV.

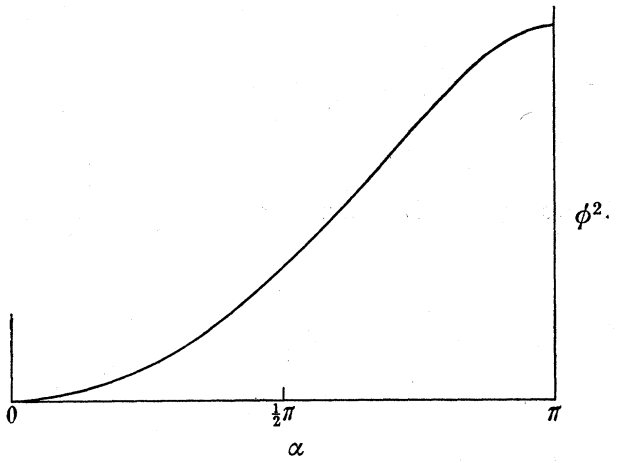

FIGURE 16. Energy-momentum curve computed from Kronig–Penney model.

It will be seen from figure 13 that between L and K the model gives a good representation of the shape of the surface found by experiment—indeed there is coincidence of the two surfaces almost as far as K, where they differ in radius vector by only $\frac{1}{2}$%. Towards X the agreement is not so good, but this would not be expected, for there is strong indication in the concavity of the experimental surface of an attraction towards the zone boundary at X. If this interpretation of the behaviour near L be adopted, the experimental surface must be modified so as to follow the broken curve near the zone boundary, and merge smoothly with it at a little distance from L. Clearly there is no difficulty in making this adjustment in such a way as to affect the experimental surface only in the immediate vicinity of L.

When one attempts to make a similar adjustment which leaves the Fermi surface not in contact with the zone boundary, it is quickly obvious that the Kronig–Penney model used will not allow a satisfactory fit. In order to get the surface near L inside the asymptotic cone a smaller value of C and correspondingly larger ratio m_t/m_n must be chosen to enlarge the semi-angle of the cone. The resulting energy surfaces do not then join smoothly on to the

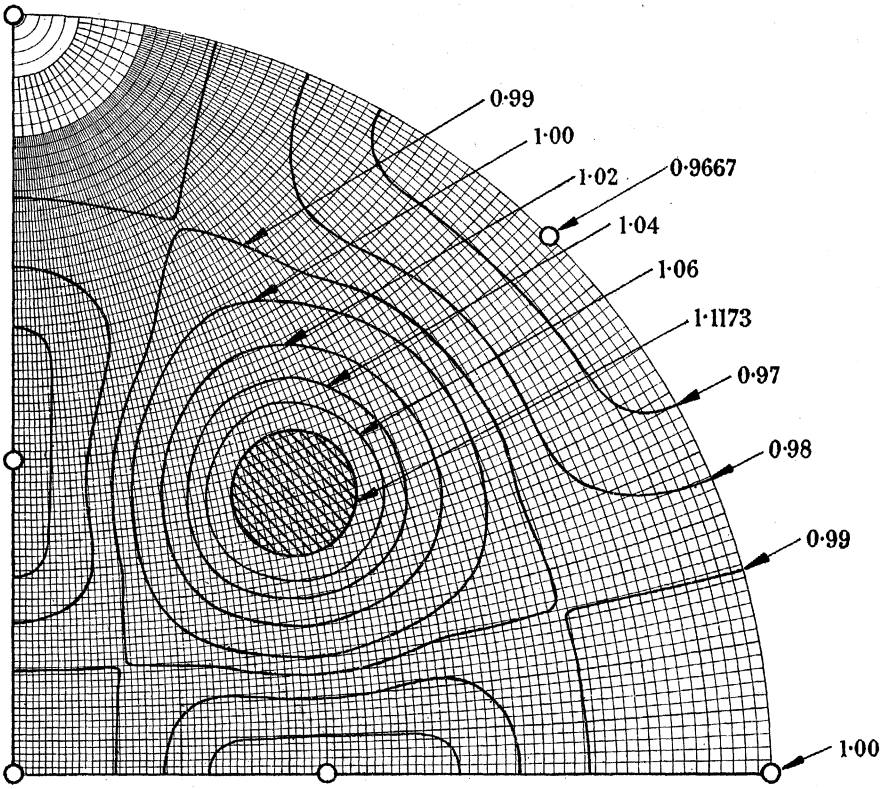

FIGURE 17. Contours of radius vector for suggested Fermi surface of copper.

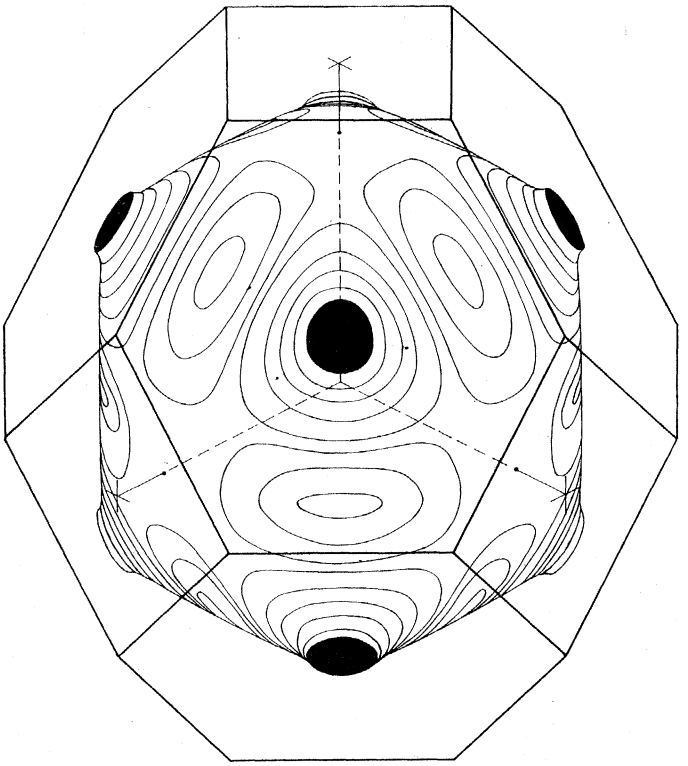

FIGURE 18. Rough drawing of surface represented more precisely by contours of figure 17.

PHILOSOPHICAL TRANSACTIONS OF THE ROYAL SOCIETY A MATHEMATICAL, PHYSICAL & ENGINEERING SCIENCES

experimental surface at a distance from L. It is difficult to assess the weight which should be given to the results of the oversimplified model, but it is likely that the general shape of the energy surfaces near a zone boundary is not very sensitive to the model, and if this is so there is no doubt that to allow contact at the boundary involves far less adjustment of the experimental surface than would be needed otherwise. It should be noted that the good fit achieved by the strict use of the Kronig–Penney model to determine both m_n and m_t may be matched by fixing m_t arbitrarily at some not too different value and choosing C differently. For example if we put $m_t=1$ and $C=1{\cdot}68$ the resulting energy surface is virtually indistinguishable from that drawn in figure 13, but the implied energy gap at L is 7·06 eV rather than 7·65 eV.

We therefore conclude, though perhaps with no very strong conviction, that the Fermi surface in copper touches the Brillouin zone boundaries in the vicinity of the (111) directions. We must now make some estimate of the change in predicted surface resistance which this modification brings about. The effect is not large, because the greater part of the eliminated surface has only a small radius of curvature. It is greatest around 55° in series 1, where the increase of R_x and R_y amounts to about 2%; this is not enough to account for the discrepant value given by specimen ζ, which is about 5% too large. It is hardly worth while adjusting the shape of the predicted curve of R_x, in view of the uncertainties in the original computations, and we may say that the experimental evidence does not preclude the possibility of contact between the Fermi surface and the zone boundary. At the same time it does not confirm contact, though one may confidently assert that if contact does not occur then the Fermi surface must run extremely close to the boundary; for otherwise the marked anisotropy of R could not be accounted for.

Since the balance of evidence favours contact, the considered final surface has been drawn to join smoothly with the broken lines in figure 13, and the result is shown in figure 17 as a contour plot on a stereographic diagram, and as a perspective drawing in figure 18. It is extremely difficult to estimate the reliability of this result. Small changes to the shape can certainly be made in regions where the curvature is high, as witness the small effect produced by contact with the boundary. On the other hand, small changes in regions of low curvature affect areas of the surface whose normals lie within a narrow pencil, and in consequence the changes are reflected as severe localized changes in R. It is doubtful whether any change in radius vector greater than 1% can be applied anywhere except near the (111) direction without worsening the agreement with experiment. There is, however, still to be answered the question whether there may not exist a totally different surface which will fit the experimental results equally well. To this the only immediate answer is that none has been discovered; moreover, it is unlikely that any other solution would accord with simple ideas about the attraction which the zone boundaries have for the Fermi surface, so well exemplified by the solution proposed here.

Discussion

Comparison with measurements at other frequencies

It is of interest to compare the present results with those obtained with copper at other frequencies, by Chambers (1952) at 1200 Mc/s and Fawcett (1955) at 36000 Mc/s, since the use of the anomalous skin effect depends on a theoretical formula, which may be tested

PHILOSOPHICAL TRANSACTIONS OF THE ROYAL SOCIETY A MATHEMATICAL, PHYSICAL & ENGINEERING SCIENCES

to some extent by the frequency variation found experimentally. Comparison is not quite straightforward, since Chambers and Fawcett both used polycrystalline specimens, and presumably measured the average value of R over all orientations. Now it was conjectured by Chambers that this average, $\bar{R}$, was related to S, the total free area of Fermi surface (i.e. all but those parts in contact with zone boundaries) by the relation

$$(\bar{R})^{-3} = 2e^2S/(3^{\frac{3}{2}}\pi\omega^2h^3). \tag{10}$$

It is more correct, however, as shown in I, to replace $(\bar{R})^{-3}$ by $\overline{(R^{-3})}$. If we are to compare the present results with those for polycrystalline specimens we must, after calculating $\overline{(R^{-3})}$ from the Fermi surface, estimate the difference between the two averages from our knowledge of the anisotropy. Graphical integration gives a value for the free area of the surface in figure 17 which is 0·990 times the area of a sphere of the same volume. This means that $\overline{(R^{-3})}$ should have 0·990 times the value which a free electron model would predict for copper; the calculated average $\overline{(R^{-3})}^{-\frac{1}{3}}$ is $9{\cdot}01\times10^{-3}\ \Omega$ at the frequency of these experiments, 22700 Mc/s, and $1{\cdot}269\times10^{-3}\ \Omega$ at 1200 Mc/s, the frequency of Chambers's experiments. The latter figure uncorrected for differences in averages agrees very well with Chambers's value of $1{\cdot}261\times10^{-3}\ \Omega$, but unfortunately a rough estimate based on the measured variation of R with orientation indicates that $\bar{R}$ should be about 3·5% greater than $\overline{(R^{-3})}^{-\frac{1}{3}}$. It may be argued, however, that this is an overestimate of the discrepancy, for as a result of working at a much lower frequency Chambers was unable to get a larger ratio of free path to skin depth than 20; this implies that the effective electrons occupied an angular range of at least $\pm13°$. It is clear from figure 11 that if R is averaged over this interval the larger excursions from the mean will be appreciably reduced and thus the difference between the two average values of R over all orientations will not be so great as the 3·5% originally estimated. It is probably fair to say that in a change of frequency by a factor of 18·9 from Chambers's to the present experiments the theoretical variation of R as $\omega^{\frac{2}{3}}$ is obeyed within 2·5%, or that if $R\propto\omega^{\alpha}$ the exponent α is probably between 0·66 and 0·68. At 36000 Mc/s, the frequency used by Fawcett, a polycrystalline sample might be expected from the present results to have a resistance of $1{\cdot}24\times10^{-2}\ \Omega$ (Fawcett's estimate of the correction to be applied for relaxation effects has been used here); the observed value was not less than $1{\cdot}31\times10^{-2}\ \Omega$. This comparison illustrates the systematic discrepancy already referred to, which is probably to be attributed to a calibration error in Fawcett's measurements, and not, in view of the comparison with Chambers's results, to any marked deficiency in the theory of the anomalous skin effect.

Density of states and electronic specific heat

The electronic contribution to the specific heat is proportional to the temperature, the constant of proportionality γ being determined by the density of states at the Fermi surface, which itself is proportional to $\int \mathrm{d}S/v_0$, v_0 being the Fermi velocity at a point on the surface, and the integral extending over the whole of the free surface. To estimate γ we must estimate v_0 and its variation over the Fermi surface, and although this cannot be done at all precisely the result of a rough calculation is not without interest. We assume that the one-dimensional model used above is adequate to describe the energy-momentum

relation in the vicinity of the point L in figure 13, where the velocity is low and the contribution to the density of states high; and we take m_t here to be 1·1066 as before. This is sufficient to define the velocity precisely so long as the model is applicable. As one proceeds along the central section of the Fermi surface towards K, v_0 must tend to an extremum, since the surface is symmetrical about ΓK; this was found by a graphical continuation of the calculated variation of v_0 near L, so that the whole variation of v_0 from L to K was determined approximately. Next an attempt was made to fix v_0 at the point X, two independent estimates being made. For the first, it was assumed that the energy-momentum relation along ΓX also followed the one-dimensional model, with the same value, 1·80, of C so as to satisfy the requirement of isotropy of effective mass at the origin Γ. This led to a value for v_0 which was $0{\cdot}623v_f$, where v_f is the velocity of a free electron with the same momentum. This calculation however is not quite self-consistent, for it is at a radius of 0·984 rather than the experimental radius of 1·000 that the energy in this model reaches the Fermi energy determined by the use of the same value of C along the direction ΓL.

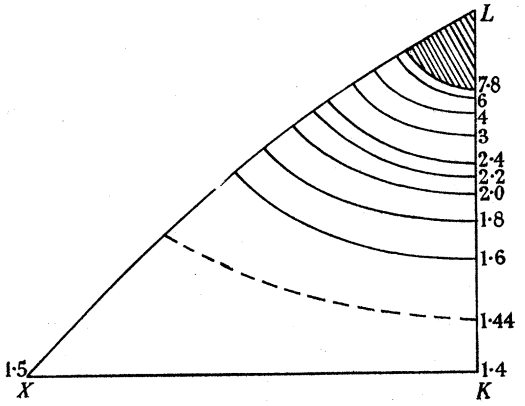

FIGURE 19. Contours of $1/v_0$.

The second estimate of v_0 at X comes from the curvature of the Fermi surface at this point, v_0 being proportional to ρ_X/m_t, where ρ_X is the radius at X and m_t is the transverse mass, taken as 1·1066. This leads to a value for v_0 which is $0{\cdot}695v_f$; but the method is very unreliable, since a very small adjustment of the surface near X could alter ρ_X noticeably without affecting the resistance appreciably. There is, however, reasonably good agreement between the two estimates, and we have taken v_0 to be $\frac{2}{3}v_f$ at this point. Finally, a contour diagram of $1/v_0$ has been constructed by graphical interpolation, the form of the contours being guided by the general consideration that v_0 is likely to be largest where the radius of the Fermi surface is smallest, since in these directions the influence of the zone boundaries, which tend to lower v_0, is least felt. The resulting diagram is shown in figure 19, and the average value of $1/v_0$, obtained by graphical integration, is 1·89 times that for a free-electron gas of the same density; this corresponds to a mean velocity of $8{\cdot}3 \times 10^7$ cm s^{-1}. If the assumption that the transverse mass at the points L and X is 1·1066 should be wrong, the estimate of $\overline{1/v_0}$ will be correspondingly wrong; for example, a choice of 1·00 for the transverse mass leads to a value of $\overline{1/v_0}$ only 1·71 times the free-electron value. It would be hard to force a much lower value than this out of the scheme presented here. Since the value of S is 0·99 times that for a free-electron gas, we arrive at a value of γ which is 1·87 times the free-electron value, γ_0, if $m_t = 1{\cdot}1066$, or 1·69 if $m_t = 1$.

The experimental value of γ, according to Corak, Garfunkel, Satterthwaite & Wexler (1955) is 6880 erg mol.$^{-1}$ deg.$^{-2}$, which is $1{\cdot}38\gamma_0$. It is in accordance with the views of Bohm & Pines (see Pines 1955), that the experimental value of γ should be rather lower than that calculated by a one-electron approximation, on account of the influence of plasma modes in reducing the degrees of freedom of the particle-like excitations of a Fermi gas. Although the theory has not been developed to the stage of being quantitatively applicable when the Fermi surface is not spherical, it is, nevertheless, interesting to estimate the order of the effect that the theory might predict. The calculated value of γ should, according to Pines (1955 (8·4)) be reduced by a factor

$$\left\{1+\frac{m^*}{m}\frac{r_s}{12{\cdot}07}[1{\cdot}47+0{\cdot}0625\,r_s-\ln r_s]\right\},$$

in which r_s is a measure of the separation of conduction electrons, taking the value 2·67 in copper, and m^*/m may be tentatively interpreted here as the ratio of the calculated γ to the free-electron value. If m_t is taken as 1·1066, we have $m^*/m=1{\cdot}87$, and the corrected value of γ is $1{\cdot}47\gamma_0$; while if m_t is taken as 1·0, $m^*/m=1{\cdot}69$, and the corrected value of γ is $1{\cdot}36\gamma_0$. There is therefore no need to suppose the calculations of γ to disagree with experiment, but the uncertainties in the calculations are such that they cannot be held to confirm either the suggested shape of the Fermi surface or the correction to γ suggested by Pines.

Transport properties, etc.

The conduction of electricity and heat in copper, and related effects such as the thermoelectric power, the Hall effect and the magnetoresistance, all pose problems if copper is regarded as very nearly a free-electron metal with a spherical Fermi surface. The relation between electrical and thermal conductivity has been discussed by Klemens (1954) who has been led to conclude that there must be contact between the Fermi surface and the zone boundary. Jones (1955) has argued that the wrong sign (compared with a free-electron metal) of the thermoelectric power does not necessarily imply contact, but at least the Fermi surface must run rather close to the zone boundary. The magnitude of the Hall effect and the absence of saturation of the transverse magnetoresistance both indicate, according to Chambers's (1956) discussion, that either the Fermi surface is not closed or the standard treatment of these effects is seriously in error.

It would be rash to claim that the present evidence for contact between Fermi surface and zone boundary removes at one stroke all difficulties in understanding the transport properties of copper. Probably the relation between electrical and thermal conduction discussed by Klemens is clarified, and there is probably no difficulty in understanding the sign of the thermoelectric power. But a full verification of these points would involve a discussion of the variation of free path over the Fermi surface, and subsequent detailed computations, all of which is a major undertaking not to be attempted here. More work still would be involved in computing the Hall effect and magnetoresistance, and all that is worth saying here is that there is no obvious resolution of the difficulties discussed by Chambers. In short, although it may be hoped that the present results will provide a starting point for a more realistic treatment of transport properties than is provided by the theoretical quasi-free model with ellipsoidal bands, there seems to be

a rather strong likelihood that the results of such a treatment will be disappointing enough to focus attention on the deficiencies in the general theory of transport phenomena, especially in the presence of a magnetic field.

Theoretical calculations of the Fermi surface

Not many calculations have been made which will yield predicted forms for the Fermi surface in copper; of these, Howarth's (1955) application of the augmented plane wave method is the most ambitious. Unfortunately, however, this work contains an error which invalidates the results (private communication from Dr Howarth), so that the marked discrepancies between his energy surfaces and that determined here are not necessarily significant. Another calculation by Howarth (1953), using the cellular method, showed that the energy gaps across the zone boundaries are very sensitive to the choice of core potential. For example, at L the gap was 0·24 eV if the Hartree Cu^+ potential was used, and 1·7 eV for the Hartree–Fock Cu^+ potential. Both these gaps are considerably smaller than that conjectured from the present results, and indeed the Fermi surface according to this calculation should be far too nearly spherical to account for the anisotropy in surface resistance.

An earlier, more empirical, approach by Jones (1937) assumed, on the basis of ultra-violet absorptivity, an energy gap of 4·1 eV at the point L, and used the approximation of almost-free electrons to calculate the shape of the energy surfaces. In so far as the results of the present work show the dominating influence of the attraction of the zone boundary at L, there is qualitative agreement with Jones's calculation; but the estimate of 4·1 eV for the gap, though greater than in Howarth's (1953) work, still seems to underestimate the attraction of the boundary. This estimate is based on a conjectural interpretation of a few rather widely spaced ultra-violet observations (Minor 1903) on heavily polished copper surfaces, which cannot be regarded as convincing evidence for the magnitude of the gap. In this connexion it may be noted that the soft X-ray spectrum of copper (Cauchois 1953) is surprisingly innocent of interpretable features, and provides no certain clue to the density of states near the Fermi surface nor to the size of the energy gaps at the zone boundaries.

We may sum up these brief comparisons by remarking on the absence of experimental information whose interpretation may be taken to confirm or cast doubt on the suggested form of the Fermi surface. It is hard to believe that the anomalous skin-effect measurements can be interpreted without supposing the Fermi surface to run extremely close to the zone boundary, even if it does not actually touch it, and the remarkable sensitivity of the thermoelectric power to small additions of other metals may be taken to support this (MacDonald & Pearson 1953). It is, however, doubtful whether very much useful information may be obtained at present from the changes in transport properties caused by addition of impurities, since these are so violent as to appear to lie outside the conventional theory of metals.

Evaluation of the method

Since this is the first application of anomalous skin-effect measurements to determine the electronic structure of a comparatively simple metal, it is worth while recording some opinions about the general usefulness of the method, particularly compared with the only

PHILOSOPHICAL TRANSACTIONS OF THE ROYAL SOCIETY A MATHEMATICAL, PHYSICAL & ENGINEERING SCIENCES

other method yet attempted, that employing the de Haas–van Alphen effect. The technical problems involved are those of preparing pure single crystals with good surfaces; they appear to have been overcome with copper, and there are quite a number of metals which should offer no greater difficulties. The microwave and cryogenic problems are trivial in comparison. The major problems are then those of interpretation. It was thought at first (see I) that the fact that the curvature of the Fermi surface entered into the expression for R as a cube root would result in only rather small anisotropies of R in simple metals, and would therefore make it necessary to achieve very high accuracy in the measurements. Present experience shows, however, that comparatively small deformations of a sphere cause such large changes of curvature that even R becomes highly anisotropic. This behaviour, while greatly enhancing the sensitivity of the method, brings computational difficulties in its train, as is illustrated in the appendix, since rough-and-ready graphical methods can lead to large errors. Perhaps this aspect should not be overstressed; there is no obstacle in principle to setting up an interpolation program for a digital computer so that corrections to an analytic form of surface could be applied smoothly and automatically. A more serious and time-consuming difficulty is that there is no known analytic procedure by which the shape of the Fermi surface can be inferred from the anisotropy of the skin resistance. A synthetic method has been used here, in which a surface is guessed and adjusted by trial and error. This limitation contrasts markedly with what is possible in the analysis of the de Haas–van Alphen effect; here, with certain not too restrictive assumptions, a complete set of experimental data may be analyzed by a systematic procedure and a unique surface deduced (Lifshitz & Pogorelov 1954; Gunnersen 1957). Important additional merits of the de Haas–van Alphen effect are, first, that the quantity measured is much more simply evaluated for a given surface than the integrals occurring in (2) and (3), and secondly, that each sheet of the Fermi surface gives its own individual periodicity, while the contributions of all sheets are combined inextricably in the surface resistance. In view of the complexity of resistive behaviour which we have seen to be possible with a single Fermi surface, it seems most unlikely that a more complex metal can be analyzed without a great deal of assistance from other methods and measurements, and this is the reason for our introductory reflexions on Fawcett's (1955) analysis of the Fermi surface in tin.

It is likely then that the anomalous skin effect may prove a useful adjunct to other studies, particularly high-field de Haas–van Alphen studies (Shoenberg 1957), but that only for the monovalent metals can it stand by itself. Since it is just these metals that have failed so far to show the de Haas–van Alphen effect, and are at the same time of most immediate interest so far as detailed structure calculations are concerned, the usefulness of the anomalous skin effect is by no means negligible, even though there are only three metals, copper silver and gold, which possess the necessary electronic simplicity and technical properties to bring out the full merits of the method.

This work was a consequence of an invitation to spend a year as visiting professor at the Institute for the Study of Metals, University of Chicago. I should like to express my deep gratitude to the Director, Professor C. S. Smith and Acting Director, Professor E. A. Long, for their hospitality, and to all members of the staff of the Institute for their help and

PHILOSOPHICAL TRANSACTIONS OF THE ROYAL SOCIETY A MATHEMATICAL, PHYSICAL & ENGINEERING SCIENCES

encouragement. More specifically I am indebted to Mr K. K. Ikeuye for the preparation of the copper crystals, to Mr V. W. Pratt for cutting and orienting the specimens, and to Mrs Betty Nielsen for her immaculate electropolishing.

The analysis of the data was carried out in Cambridge, and I must acknowledge the invaluable help provided by the Mathematical Laboratory, and particularly by Dr C. B. Haselgrove and Mrs Margaret Mutch. I am also grateful to Mr R. W. Horne for his electron-micrographical examination of one of the specimens. Finally, it is a pleasure to record my debt to Professor Harvey Brooks, Dr J. M. Ziman and Dr R. G. Chambers for many valuable discussions.

References

Cauchois, Y. 1953 *Phil. Mag.* **44**, 173.
Chambers, R. G. 1952 *Proc. Roy. Soc.* A. **215**, 481.
Chambers, R. G. 1953 *Physica*, **19**, 365.
Chambers, R. G. 1956 *Proc. Roy. Soc.* A, **238**, 344.
Corak, W. S., Garfunkel, M. P., Satterthwaite, C. B. & Wexler, A. 1955 *Phys. Rev.* **98**, 1699.
Dingle, R. B. 1953 *Physica*, **19**, 311.
Fawcett, E. 1955 *Proc. Roy. Soc.* A, **232**, 519.
Gunnersen, E. M. 1957 *Phil. Trans.* A, **249**, 299.
Howarth, D. J. 1953 *Proc. Roy. Soc.* A, **220**, 513.
Howarth, D. J. 1955 *Phys. Rev.* **99**, 469.
Jones, H. 1937 *Proc. Phys. Soc.* **49**, 250.
Jones, H. 1955 *Proc. Phys. Soc.* A. **68**, 1191.
Kaganov, M. I. & Azbel′ M. Ya. 1955 *Dokl. Akad. Nauk SSSR*, **102**, 49.
Klemens, P. G. 1954 *Aust. J. Phys.* **7**, 70.
Kronig, R. de L. & Penney, W. G. 1930 *Proc. Roy. Soc.* A, **130**, 499.
Lifshitz, I. M. & Pogorelov, A. V. 1954 *Dokl. Akad. Nauk SSSR*, **96**, 1143.
Macdonald, D. K. C. & Pearson, W. B. 1953 *Proc. Roy. Soc.* A. **219**, 373.
Minor, R. S. 1903 *Ann. Phys., Lpz.*, **10**, 581.
Pines, D. 1955 *Solid State Phys.* **1**, 367.
Pippard, A. B. 1954 *Proc. Roy. Soc.* A, **224**, 273.
Reuter, G. E. H. & Sondheimer, E. H. 1948 *Proc. Roy. Soc.* A, **195**, 336.
Shoenberg, D. 1957 *Progr. Low Temp. Phys.* **2**, 226.
Sondheimer, E. H. 1954 *Proc. Roy. Soc.* A, **224**, 260.

Appendix

In this appendix are noted briefly the computational methods used for applying a graphical correction to the analytical form of Fermi surface. The labour involved arises from the fact that for some parts of the calculations Cartesian co-ordinates are employed while for others polar co-ordinates are the natural choice. The specification of an analytical form of surface in Cartesian co-ordinates, as (4), enables plane sections at constant y to be made, and curvatures and normals tabulated automatically, with least waste of machine time; on the other hand, to apply a correction to this surface graphically, while still maintaining cubic symmetry, is most readily done by plotting corrections to the radius vector Δr, as a function of latitude ϑ and longitude ϖ on a stereographic chart, as in figure 10.

Given $\Delta r\ (\vartheta, \varpi)$, we wish to calculate the changes produced in the radius of curvature ρ_y and inclination of the normal θ in sections of constant y. The first step is to calculate the change $\Delta r'$ of the radius vector in the plane $y=$constant. The relation between the different co-ordinate systems is shown in figure 20. P is a point (x, y, z) or (r, ϑ, ϖ) on the unmodified surface of which LPM is a chord. PN is drawn parallel to the XZ plane

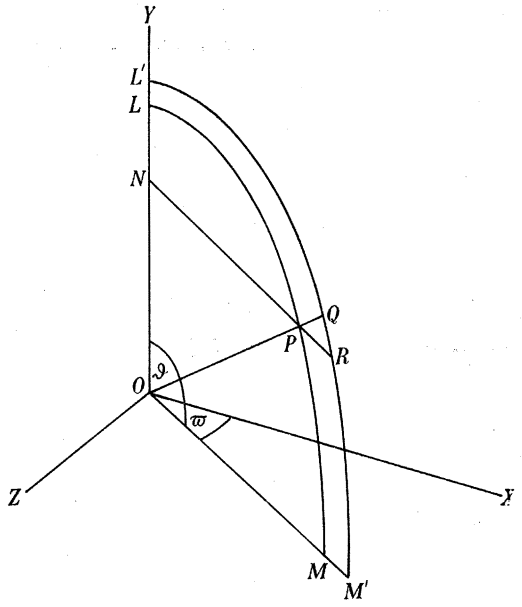

FIGURE 20. To show notation.

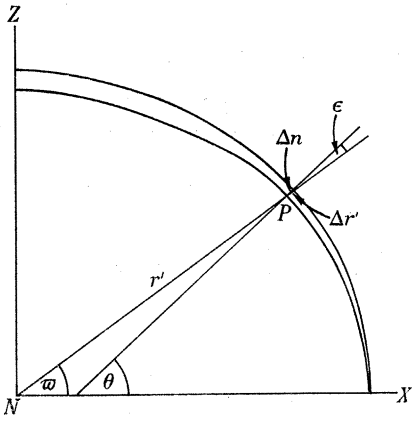

FIGURE 21. Section of surface by plane $y=$constant.

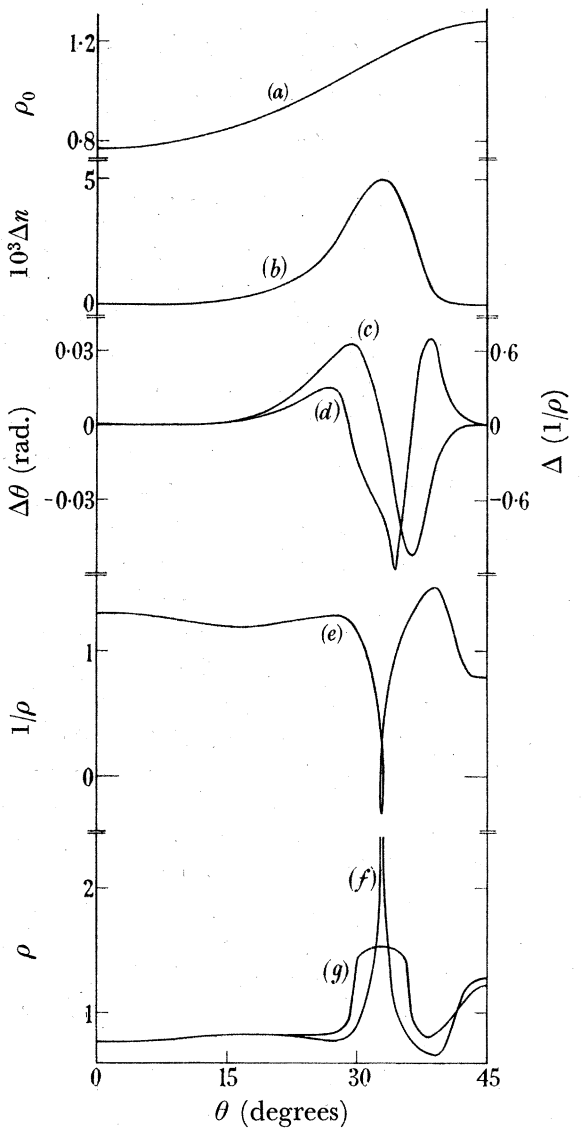

FIGURE 22. Stages in computing corrections to θ and ρ; see text for description.

and represents r', the radius vector in the plane $y=ON$; in this plane P is described by the co-ordinates (r', ϖ). If now $L'QRM'$ is the modified form of the chord LPM, PQ is Δr and PR is $\Delta r'$, and $\Delta r'$ sin $\widehat{PRQ}=\Delta r$ sin $\widehat{PQR}$. The angles $\widehat{PRQ}$ and $\widehat{PQR}$ are calculated as functions of ϑ and ϖ for the unmodified surface, and a stereographic chart thus constructed showing $\Delta r'/\Delta r$ for all parts of the surface. This enables the correction $\Delta r'$ to be found for any choice of correction Δr, such as that in figure 10.

We now turn our attention to a section of the surface at constant y, as in figure 21 where unmodified and modified sections are represented schematically. From the tabulations of the unmodified surface the variation of ϵ with ϖ is known, ϵ being the angle between the radius vector r' and the normal to the surface; ϵ is in fact $\theta-\varpi$. It is therefore possible to plot a graph of $\Delta n\ (=\Delta r' \cos\epsilon)$ against θ. Now because Δn varies along the curve both the direction of the normal and the radius of curvature are changed by the corrections. If θ is the change in direction of the normal, $\Delta\theta = \mathrm{d}(\Delta n)/\mathrm{d}s$, where s is distance measured along the curve. But $\mathrm{d}\theta/\mathrm{d}s = 1/\rho_0$, where ρ_0 is the radius of curvature of the unmodified surface in the section of figure 21, and is a tabulated function of θ; therefore

$$\Delta\theta = \frac{1}{\rho_0}\frac{\mathrm{d}}{\mathrm{d}\theta}(\Delta n),$$

and hence by a single graphical differentiation the correction $\Delta\theta$ is deduced. To find the change in curvature we note that

$$\Delta\left(\frac{1}{\rho}\right) = \frac{\mathrm{d}^2}{\mathrm{d}s^2}(\Delta n) = \frac{1}{\rho_0^2}\frac{\mathrm{d}^2}{\mathrm{d}\theta^2}(\Delta n) - \frac{1}{\rho_0^3}\frac{\mathrm{d}\rho_0}{\mathrm{d}\theta}\frac{\mathrm{d}}{\mathrm{d}\theta}(\Delta n).$$

The corrections to ρ thus involve a second differentiation of the Δn–θ curve and a differentiation of the ρ_0–θ curve. This means that very considerable care is required in reading off values of Δr from figure 10, and in processing them graphically, if results are to be meaningful. A useful check on accuracy is that the area under the modified ρ–θ curve should be very nearly the same as under the unmodified curve, since $\int \rho \mathrm{d}\theta$ is simply s, the length of the curve in figure 20, and this is hardly changed by the small corrections.

As an example of the effects produced by the corrections of figure 10, we show diagrams constructed for the central section ($y=0$) of the Fermi surface normal to a cube axis. Figure 22 (a) shows the smooth variation of ρ_0 with θ in the unmodified surface, figure 22 (b) the correction Δn, figures 22 (c) and (d) the curves for $\Delta\theta$ and $\Delta(1/\rho)$ constructed by graphical differentiation, and 22 (e) the modified form of $1/\rho$ as a function of the modified θ. It will be seen from this that the corrections have caused a slight concavity to appear in the surface. Figure 22 (f) shows how ρ now varies with θ, while 22 (g) is obtained by averaging ρ over $\pm 3\frac{1}{2}^\circ$, in accordance with the ideas expounded in the text. This example is by no means extreme; for some sections corresponding to series 1 the resulting curve for ρ after correction is entirely different from that for ρ_0, even for so small a correction as that actually applied here.

PHILOSOPHICAL TRANSACTIONS OF THE ROYAL SOCIETY A MATHEMATICAL, PHYSICAL & ENGINEERING SCIENCES